Phase equilibria modeling of Cross-Associating systems guided by a quantum chemical Multi-Conformational framework

Grigorash, Daria; Mihrin, Dmytro; Wugt Larsen, René; Stenby, Erling H.; Yan, Wei

Published in:
Chemical Engineering Science

Link to article, DOI:
10.1016/j.ces.2023.119404

Publication date:
2023

Document Version
Publisher's PDF, also known as Version of record

Chemical Engineering Science 284 (2024) 119404

Contents lists available at ScienceDirect

Chemical Engineering Science

journal homepage: www.elsevier.com/locate/ces

Phase equilibria modeling of cross-associating systems guided by a quantum chemical multi-conformational framework

Daria Grigorash [a,b], Dmytro Mihrin [a,c], René Wugt Larsen [a], Erling H. Stenby [a,b], Wei Yan [a,b,*]

[a] Department of Chemistry, Technical University of Denmark, 2800 Kgs. Lyngby, Denmark
[b] Center for Energy Resources Engineering (CERE), Technical University of Denmark, 2800, Kgs. Lyngby, Denmark
[c] Danish Offshore Technology Centre, Technical University of Denmark, 2800 Kgs. Lyngby, Denmark

ARTICLE INFO

Keywords:
Cross-association
Quantum chemical calculation
Phase equilibrium
Equations of state
Cubic-Plus-Association

ABSTRACT

Cross-association between molecules may result in several conformations of weakly bound molecular complexes with different association energies. However, the conventional combining rules used in equations of state account only for one conformation. Therefore, in the present work we introduce a framework that allows one to distinguish the cross-interactions between sites of different nature and to expand the number of captured conformations coexisting in the mixture. We incorporated the proposed approach into the Cubic-Plus-Association (CPA) equation of state and applied it to model the binary Vapor-Liquid Equilibrium (VLE) of aqueous mixtures with alcohols (methanol, ethanol, propan-2-ol, *tert*-butanol, and phenol), acetic acid, and CO_2. For the mixtures with alcohols, we report the quantum chemical association energies calculated with the benchmark Domain-Based Local Pair Natural Orbital Coupled-Cluster Single, Double, and Perturbative Triple DLPNO-CCSD (T) approach and compare these values with association energies obtained by fitting to experimental data using a distinguishable interactions approach. Based on the updated results for the binary systems, we investigated how the new cross-association parameters will affect the predictions of the ternary Liquid-Liquid Equilibrium (LLE) of water–alcohol–hydrocarbon mixtures and VLE of water–acetic acid–CO_2 mixtures.

1. Introduction

In recent decades the Statistical Associating Fluid Theory (SAFT) family of equations of state (EoSs) has become a benchmark in the thermodynamic modeling of associating mixtures. These rapidly developing models are based on Wertheim's first-order thermodynamic perturbation theory (TPT1) (Wertheim, 1984; Wertheim, 1984; Wertheim, 1986; Wertheim, 1986) and share almost the same association term derived from TPT1 by Chapman et al. (Chapman et al., 1988; Jackson et al., 1988). Approximations in the derivation of the theory simplify intermolecular interactions in real mixtures by neglecting steric hindrance, cooperativity, and multiple bonding. Since the inception of this theory, several extensions have been proposed to overcome some of its limitations. Hydrogen bond cooperativity has been extensively investigated (Sear and Jackson, 1996; Marshall and Chapman, 2013; Marshall, 2017; Marshall, 2019). Furthermore, steric hindrance and ring formation have been considered within the perturbation theory framework (Marshall et al., 2014; Haghmoradi and Chapman, 2019). In addition, the extension of the perturbation theory approach to capture intramolecular hydrogen bond interactions has also been developed (Avlund et al., 2011). The introduced modifications expand the range of physical effects in real mixtures captured by the SAFT models. However, they come at the cost of increased mathematical complexity, while the model performance is still highly dependent on parameter estimation.

The most widely studied type of association at both macroscopic and microscopic scales is hydrogen bonding (HB), which is the main, although not the only focus of SAFT modeling. Hydrogen bonding is an attractive interaction between atoms with a significant difference in electronegativity, e.g., the atoms of H and O, N, and F, and has been widely studied at both macroscopic and microscopic scales. Modern spectroscopic methods and high-level quantum chemical (QC) calculations provide valuable insights into hydrogen bond characteristics. Using these methods, one can estimate the strength of the intermolecular bond formation and predict the geometry of associated molecular complexes. SAFT-type EoSs can benefit from microscopic inputs since its association parameters have well-defined physical meanings that are related to molecular characteristics. Wolbach et al. (Wolbach and Sandler, 1997; Wolbach and Sandler, 1997; Wolbach and Sandler, 1997;

* Corresponding author at: Department of Chemistry, Technical University of Denmark, 2800 Kgs. Lyngby, Denmark.
E-mail address: weya@kemi.dtu.dk (W. Yan).

https://doi.org/10.1016/j.ces.2023.119404
Received 17 May 2023; Received in revised form 30 September 2023; Accepted 14 October 2023
Available online 16 October 2023

Wolbach and Sandler, 1998) and Towne et al. (Towne et al., 2021) integrated QC predictions in estimating the association energy and volume for pure substances with the SAFT (Chapman et al., 1989; Chapman et al., 1990), PC-SAFT (Perturbed Chain SAFT) (Gross and Sadowski, 2001), and CPA (Cubic-Plus-Association) (Kontogeorgis et al., 1996) EoSs. The reported results demonstrate a decent agreement between the association energies obtained via fitting thermodynamic experimental data and those from theoretical QC calculations. Thus, consideration of studies on microscopic properties of molecules in SAFT modeling is highly promising. Spectroscopic measurements detecting hydrogen-bonded molecular complexes are also involved in the parametrization and validation of the SAFT-type models. Von Solms et al. (Von Solms et al., 2006) used experimental data on the monomer fraction of pure associating fluids in selecting the appropriate association scheme and also incorporated these data in the regression of the pure component parameters.

In addition to pure component energies, we could benefit from theoretical input for cross-associating complexes between two distinct species. The current standard approach in cross-association modeling is based on combining rules that, by means of simple algebraic equations, relate pure component association energies to mixed dimer values. However, modern spectroscopic and QC studies show that conformations of molecular dimers formed with different types of association sites can bind with non-identical association energies, which are not accounted for in the conventional combining rule approaches. IR (Infrared) spectroscopy combined with theoretical calculations from *first principles* quantum chemistry can be used to determine the semi-experimental zero-point energy (ZPE) corrected dissociation energies with high accuracy. Several binary hydrogen-bonded water–alcohol systems with methanol, ethanol, propan-2-ol, and *tert*-butanol (Nedić et al., 2011; Andersen et al., 2015; Andersen et al., 2015) have been investigated with these techniques. The obtained results indicate two stable conformations of a series of water–alcohol dimers with non-identical association energies. One conformation of these water–alcohol dimers is formed through the H-atom of the water molecule (positive site), whereas the second conformation engages the O-atom on the water molecule (negative site). It should be noted that the indicated difference in the conformational interaction energies of cross-associating dimers is not accounted for in the conventional combining rule approaches. Nevertheless, it is possible to distinguish the specific interactions and to use different association energies or association strengths for conformations formed with sites of different natures within the SAFT approach. The ZPE-corrected dissociation energies may serve as a direct input for the model or as guideline for the fitting procedure to obtain distinguishable interaction (DI) energies. Applications of this approach might include both hydrogen-bonded and more weakly van der Waals solvated complexes. It is worth noting that specific cross-interactions have already been investigated in some previous studies. For instance, specific conformations of molecular complexes were considered in modeling the solvation between water and benzene (Kontogeorgis et al., 2008) or CO_2 (Tsivintzelis et al., 2011) with the CPA EoS: the former results in a non-conventional hydrogen bond interaction between the π-electrons of the benzene ring and the H-atom of water, whereas the latter is formed via a weaker van der Waals interaction involving the O-atom of water and the C-atom of CO_2. Studies on the phase equilibria modeling of alkanolamines in SAFT-VR (Mac Dowell et al., 2010; Rodriguez et al., 2012) suggest the use of an asymmetric approach where multifunctional groups are identified and their cross-association parameters are treated separately. Distinguishable interactions are also used in the SAFT-γ Mie group-contribution EoS for cross-associating compounds (Dufal, 2014; Haslam, 2020). The group cross-association parameters are fitted to experimental data instead of applying combining rules, which leads to greater flexibility of the model.

The major focus of the present work is to develop a cross-association modeling approach that can handle conformations with different types of site-to-site interactions separately by acknowledging the differences in their association energy. To establish the new framework, we modify the most common combining rules, namely ECR (Elliott Combining Rule) (Suresh and Elliott, 1992) and CR-1 (Combining Rule-1) (Voutsas et al., 1999), by introducing two correction factors that correspond to the two different conformations where water is bound via either its positive sites or its negative sites. We apply these modifications to the CPA EoS, although the procedure could also be implemented in other SAFT-type EoS. Then, we assess the performance of the DI approach by modeling the binary VLE for aqueous hydrogen-bonded systems with alcohols (methanol, ethanol, propan-2-ol, *tert*-butanol, and phenol) and acetic acid. In addition to hydrogen-bonded dimers, we also investigate the weakly van der Waals solvated system water–CO_2. The results obtained for these binary systems are then used to calculate ternary phase equilibria of the water–alcohol–hydrocarbon mixtures and water–acetic acid–CO_2 mixtures.

2. Methods

In the *Thermodynamic Modeling* section, we briefly review the CPA EoS and its conventional implementation for cross-associating systems. Then in the *Combining Rules* section we introduce the modifications of the existing combining rules and the regression method considered in this study. In the *Quantum Chemical (QC) Predictions of Intermolecular Potential Energy Minima* section, we present the details on the computational and experimental procedures involved in the determination of association energies between hydrogen-bonded molecules.

2.1. Thermodynamic modeling

2.1.1. CPA EoS

The CPA EoS combines the physical term of the Soave-Redlich-Kwong (SRK) EoS with the Wertheim association term, resulting in the following pressure explicit equation:

$$P = \frac{RT}{V_m - b} - \frac{\alpha(T)a_0}{V_m(V_m + b)} - \frac{1}{2}\frac{RT}{V_m}\left(1 + \rho\frac{\partial \ln g}{\partial \rho}\right)\sum_i x_i \sum_{A_i}(1 - X_{A_i}) \tag{1}$$

The physical term from the SRK EoS consists of the first two terms, where V_m is the molar volume, b is the covolume parameter, and $\alpha(T)a_0$ is the energy parameter. The a_0 parameter is temperature independent and $\alpha(T)$ is a function of temperature with a substance-dependent parameter c_1. The last term, representing the site-to-site associations, is expressed through the mole fraction of unbounded sites of type A in a molecule i, as given by the following equation:

$$X_{A_i} = \frac{1}{1 + \rho\sum_j x_j \sum_{B_j} X_{B_j}\Delta^{A_iB_j}} \tag{2}$$

where $\Delta^{A_iB_j}$ is the association strength between two sites A and B on molecules i and j, respectively. This is a function of the association energy ($\varepsilon^{A_iB_j}$), association volume ($\beta^{A_iB_j}$), and temperature (T):

$$\Delta^{A_iB_j} = g(\rho)\left[\exp\left(\frac{\varepsilon^{A_iB_j}}{RT}\right) - 1\right] b_{ij}\beta^{A_iB_j} \tag{3}$$

where $g(\rho)$ is the simplified-hard sphere radial distribution function (Kontogeorgis et al., 1999) dependent on the molar density of the system (ρ):

$$g(\rho) = \frac{1}{(1 - 1.9\eta)}, \quad \eta = \frac{1}{4}b\rho \tag{4}$$

and b_{ij} is the arithmetic mean of the covolume parameters of molecules i and j.

To perform calculations with CPA, five pure component parameters are used: a_0, b, and c_1, as required by the physical term, and $\varepsilon^{A_iB_j}$ and

Fig. 1. Illustration of the association scheme nomenclature (Huang and Radosz, 1991) with the cases considered in this study. Positive sites are colored in blue and negative sites in red; 1A represents a bipolar site (red and blue).

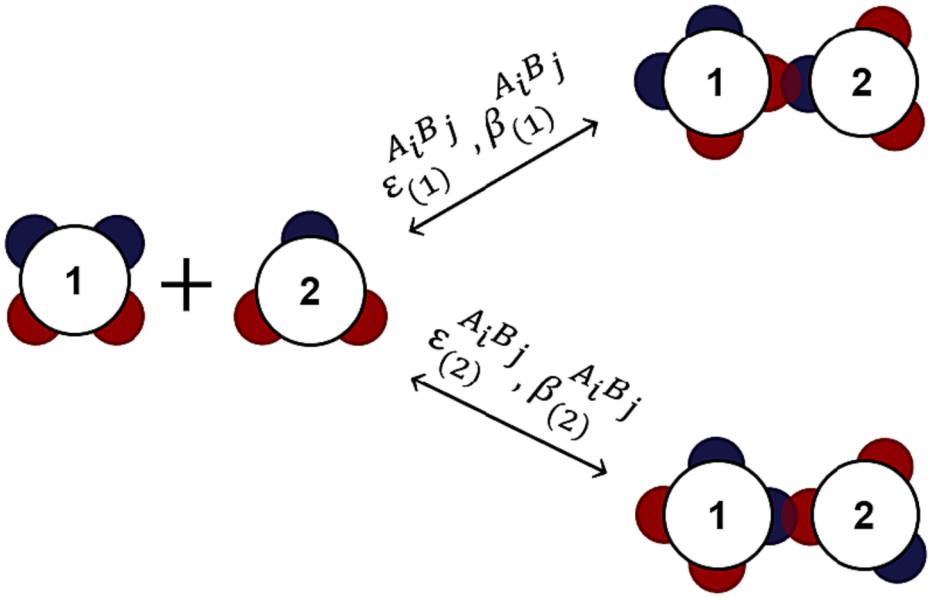

Fig. 2. The scheme of cross-association between molecules 1 (4C scheme) and 2 (3B scheme) resulting in the formation of two types of conformers. Positive sites are colored in blue and negative sites in red.

$\beta^{A_iB_j}$, as required by the association term. Conventionally, these parameters are fitted to experimental thermodynamic data on saturated vapor pressure and saturated liquid density of a corresponding substance.

Prior to the application of CPA or any other SAFT EoS, it is necessary to establish an association scheme that predetermines the nature (positive, negative, or bipolar) and number of sites. The nomenclature proposed by Huang and Radosz (Huang and Radosz, 1991) illustrated in Fig. 1 is widely used for the association scheme definition. The choice of a scheme is not a strictly established procedure. It is generally based on the user's interpretation of the association between molecules, where the molecular structure, the occurrence of steric hindrance, and the observations from spectroscopic data (Von Solms et al., 2006) play a role.

2.1.2. Combining rules

To describe the association in a mixture, we need to account for self-association as well as cross-association. The former is determined by the pure component parameters. The latter requires additional knowledge on the association between two molecules. The classical treatment for cross-association is via combining rules that relate the parameters of pure components to the binary interactions between the sites on two different molecules. Among various combining rules, the CR-1 and ECR rules appear to be the most popular (Voutsas et al., 1999; Suresh and Elliott, 1992). According to CR-1 (Eqs. (5)–(6)), the cross-association energy is calculated as the arithmetic mean of the corresponding pure component parameters and the association volume as the geometric mean:

$$\varepsilon^{A_iB_j} = \frac{\varepsilon^{A_iB_i} + \varepsilon^{A_jB_j}}{2} \tag{5}$$

$$\beta^{A_iB_j} = \sqrt{\beta^{A_iB_i}\beta^{A_jB_j}} \tag{6}$$

ECR calculates the cross-association strength as the geometric mean of the individual self-association strengths:

$$\Delta^{A_iB_j} = \sqrt{\Delta^{A_iB_i}\Delta^{A_jB_j}} \tag{7}$$

To account for the distinguishable cross-interactions characterized by different association energies, we introduce modifications to both CR-1 and ECR and refer to the modified versions as the corresponding combining rules with distinguishable interactions (DI), i.e., CR1-DI and ECR-DI, respectively.

As an illustration of the DI approach, we consider two associating compounds as shown in Fig. 2. Positive (electron acceptor) and negative (electron donor) associating sites are colored in blue and red, respectively. The number and types of sites on molecules 1 and 2 depict the 4C and 3B schemes, respectively. Cross-association can lead to the formation of two types of conformers, which differ by the nature of binding sites. In the first case ($\varepsilon_{(1)}^{A_iB_j}$) the bond is formed through a negative site on molecule 1 and a positive site on molecule 2, whereas in the second case ($\varepsilon_{(2)}^{A_iB_j}$) it is *vice versa*. We account for the different interactions between two conformers using the correction factors $m_{(1)}^{A_iB_j}$ and $m_{(2)}^{A_iB_j}$ for CR1-DI, and $M_{(1)}^{A_iB_j}$ and $M_{(2)}^{A_iB_j}$ for ECR-DI. The equations for CR1-DI are given by Eqs. (8)–(10) and those for ECR-DI by Eqs. (11)–(12).

$$\varepsilon_{(1)}^{A_iB_j} = \frac{\varepsilon^{A_iB_i} + \varepsilon^{A_jB_j}}{2} m_{(1)}^{A_iB_j} \tag{8}$$

$$\varepsilon_{(2)}^{A_iB_j} = \frac{\varepsilon^{A_iB_i} + \varepsilon^{A_jB_j}}{2} m_{(2)}^{A_iB_j} \tag{9}$$

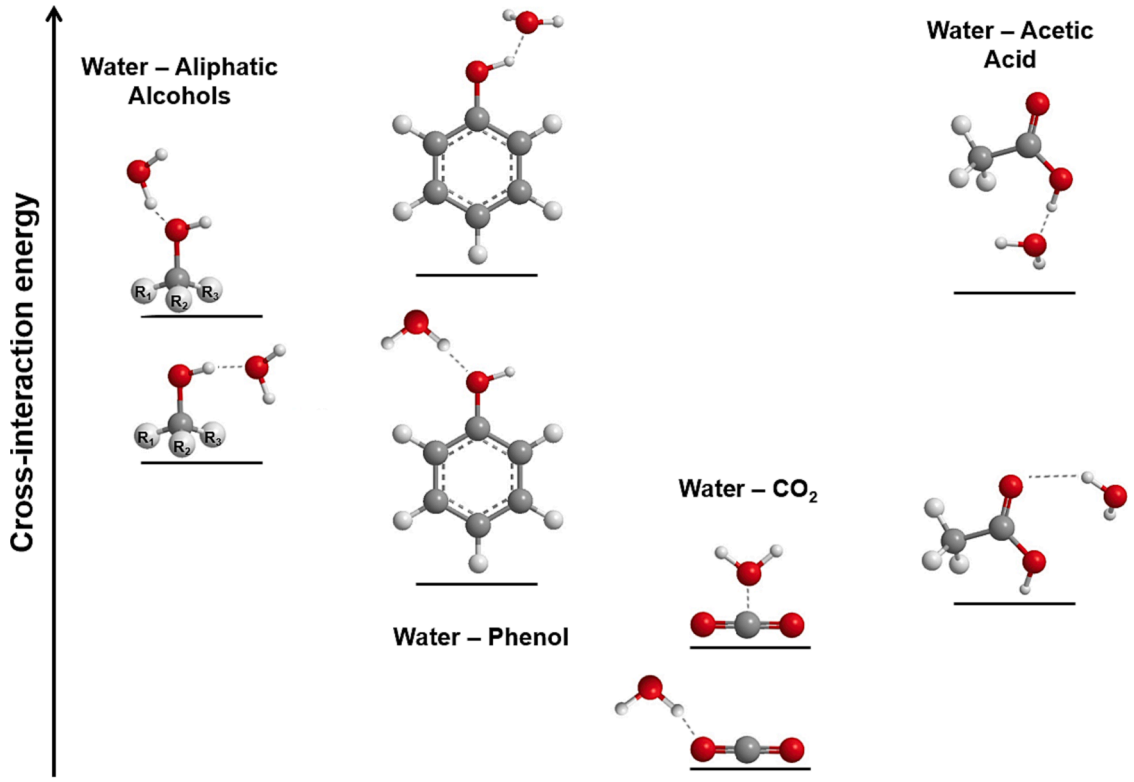

Fig. 3. Energy diagram of the different conformers of the investigated binary systems.

$$\beta^{A_iB_j}_{(1)} = \beta^{A_iB_j}_{(2)} = \sqrt{\beta^{A_iB_i}\beta^{A_jB_j}} \tag{10}$$

$$\Delta^{A_iB_j}_{(1)} = M^{A_iB_j}_{(1)}\sqrt{\Delta^{A_iB_i}\Delta^{A_jB_j}} \tag{11}$$

$$\Delta^{A_iB_j}_{(2)} = M^{A_iB_j}_{(2)}\sqrt{\Delta^{A_iB_i}\Delta^{A_jB_j}} \tag{12}$$

Currently we do not distinguish cross-association volumes, although the approach can in principle be extended to reflect this difference. Although these modifications are applied to the CPA EoS, these modified combining rules could also be used with other SAFT-type EoSs.

The relation between CR-1 and ECR has already been discussed in the analysis of these combining rules (Kontogeorgis and Folas, 2009). With the approximations $g(\rho) = 1$ and $\exp\left(\frac{\varepsilon^{A_iB_j}}{RT}\right) \geqslant 1$ the association strength according to Eq. (3) can lead to the following approximation:

$$\varepsilon^{A_iB_j} = \frac{\varepsilon^{A_iB_i} + \varepsilon^{A_jB_j}}{2} \tag{13}$$

$$\beta^{A_iB_j} = \frac{\sqrt{b_ib_j}}{b_{ij}}\sqrt{\beta^{A_iB_i}\beta^{A_jB_j}} \tag{14}$$

Eq. (13) is the same as the CR-1 rule for the association energy, while Eq. (14) is close to the CR-1 and exactly the same if $b_i = b_j$. Therefore, under certain conditions the ECR is almost equivalent to the CR-1 rule.

Likewise, we can analyze the proposed CR1-DI and ECR-DI and establish the relation between the $M^{A_iB_j}_{(1)}$ and $M^{A_iB_j}_{(2)}$ parameters of ECR-DI and the cross-association energies $\varepsilon^{A_iB_j}_{(1)}$ and $\varepsilon^{A_iB_j}_{(2)}$ of CR1-DI.

If we combine Eqs. (3) and (11), we obtain:

$$\begin{aligned}\Delta^{A_iB_j}_{(1)} &= M^{A_iB_j}_{(1)}\sqrt{\Delta^{A_iB_i}\Delta^{A_jB_j}} = M^{A_iB_j}_{(1)} \times g(\rho) \times \exp\left(\frac{\varepsilon^{A_iB_i}}{2RT}\right) \times \exp\left(\frac{\varepsilon^{A_jB_j}}{2RT}\right)\sqrt{b_ib_j}\sqrt{\beta^{A_iB_i}\beta^{A_jB_j}} = \\ &= M^{A_iB_j}_{(1)} \times g(\rho) \times \exp\left(\frac{\varepsilon^{A_iB_i} + \varepsilon^{A_jB_j}}{2RT}\right)\sqrt{b_ib_j}\sqrt{\beta^{A_iB_i}\beta^{A_jB_j}} = \\ &= g(\rho) \times \exp\left(\frac{\varepsilon^{A_iB_i} + \varepsilon^{A_jB_j}}{2RT} + \ln M^{A_iB_j}_{(1)}\right)\sqrt{b_ib_j}\sqrt{\beta^{A_iB_i}\beta^{A_jB_j}}.\end{aligned} \tag{15}$$

Then the following equality can be implied:

$$\frac{\varepsilon^{A_iB_i} + \varepsilon^{A_jB_j}}{2RT} + \ln M^{A_iB_j}_{(1)} = \frac{\varepsilon^{A_iB_j}_{(1)}}{RT} \tag{16}$$

Therefore,

$$\begin{aligned}M^{A_iB_j}_{(1)} &= \exp\left(\frac{2\varepsilon^{A_iB_j}_{(1)} - \varepsilon^{A_iB_i} - \varepsilon^{A_jB_j}}{2RT}\right) = \exp\left(\frac{\left(m^{A_iB_j}_{(1)} - 1\right)\left(\varepsilon^{A_iB_i} + \varepsilon^{A_jB_j}\right)}{2RT}\right) \\ &= \exp\left(\frac{\left(m^{A_iB_j}_{(1)} - 1\right)\varepsilon^{A_iB_j}}{RT}\right)\end{aligned} \tag{17}$$

Table 1
CPA parameters for pure components.

	a_0 (bar•l^2/mol^2)	b (l/mol)	c_1	$\varepsilon^{A_iB_j}_{(1)}$ (bar•l/mol)	$\beta^{A_iB_j}\times10^3$	Association scheme	Source
Water	1.2277	0.0145	0.6736	166.55	69.20	4C	(Kontogeorgis et al., 1999)
Methanol	4.5897	0.0334	1.0068	160.70	34.40	3B	(Kontogeorgis et al., 2006)
Ethanol	8.5755	0.0500	1.0564	150.00	17.30	3B	(Kontogeorgis et al., 2006)
Propan-2-ol	10.6019	0.0641	0.9468	210.00	9.10	2B	(Folas et al., 2005)
Propan-2-ol	11.0075	0.0651	1.0536	171.00	8.67	3B	this work[a]
tert-Butanol	16.7972	0.0816	0.8198	233.00	0.77	2B	(Tsvintzelis, et al., 2012)
tert-Butanol	16.8233	0.0820	0.8910	200.00	0.81	3B	this work[a]
Phenol	18.8400	0.0801	0.9087	174.88	45.3	2B	(Kontogeorgis et al., 2008)
Phenol	19.0157	0.08113	0.91239	157.04	29.00	3B	this work[a]
Acetic acid	9.1196	0.0468	0.4644	403.23	4.50	1A	(Derawi et al., 2004)
Acetic acid	7.0592	0.0478	0.8808	188.14	140.8	2B	(Derawi et al., 2004)
CO_2	3.5079	0.0272	0.7602				(Tsivintzelis et al., 2011)
CO_2	3.3919	0.0277	0.7575	46.2	22.61	2B	this work[a]
CO_2	2.6911	0.0273	0.5560	78.12	56.80	2B	(Tsivintzelis et al., 2011)

[a] *AARD* (Absolute Average Relative Deviation) between experimental and calculated saturated pressures or liquid densities estimated with pure component parameters regressed in this work: CO_2: $AARD(P^{sat}) = 1$ %, $AARD(\rho^{liq}) = 0.75$ %; Propan-2-ol: $AARD(P^{sat}) = 0.2$ %, $AARD(\rho^{liq}) = 0.6$ %; *tert*-Butanol: $AARD(P^{sat}) = 0.8$ %, $AARD(\rho^{liq}) = 1$ %; Phenol: $AARD(P^{sat}) = 1.8$ %, $AARD(\rho^{liq}) = 0.6$ %.

and similarly:

$$M^{A_iB_j}_{(2)} = \exp\left(\frac{\left(m^{A_iB_j}_{(2)} - 1\right)\varepsilon^{A_iB_j}}{RT}\right) \tag{18}$$

Eqs. (17)–(18) establish the relation between the correction factors of CR1-DI and ECR-DI, and, therefore, demonstrate a similarity of the two approaches analogously to the corresponding original combining rules. The binary correction factors were obtained by fitting to binary VLE data of aqueous mixtures with alcohols (methanol, ethanol, propan-2-ol, and *tert*-butanol) and acetic acid, as well as the solubility data for the water–CO_2 system. The following objective functions (*OF*) were minimized:

$$OF = \sum_{i=1}^{NP_1} w_i\left(\frac{P_i^{exp.} - P_i^{calc.}}{P_i^{exp.}}\right)^2 + \sum_{i=1}^{NP_2} w_i\left(y_i^{exp.} - y_i^{calc.}\right)^2 \tag{19}$$

$$OF = \sum_{i=1}^{NP_1} w_i\left(x_i^{exp.} - x_i^{calc.}\right)^2 + \sum_{i=1}^{NP_2} w_i\left(y_i^{exp.} - y_i^{calc.}\right)^2 \tag{20}$$

where w_i are the weights assigned to the data points; subscripts "exp" and "calc" denote experimental and calculated data, respectively, x_i and y_i liquid and vapor mole fractions, respectively, P_i the bubble point pressure. For the regression of the binary VLE data of aqueous mixtures with alcohols or acetic acid, we used Eq. (19), while for the regression of the water–CO_2 solubility data, we used Eq. (20).

2.2. Quantum chemical (QC) predictions of intermolecular potential energy minima

Quantum chemical calculations were carried out employing the ORCA (ver. 5.0) software code (Neese, Jan. 2018). Global and local intermolecular potential energy minima geometries were optimized, and the corresponding harmonic vibrational energies were predicted for two different conformations of the series of hydrogen-bonded alcohol–water molecular complexes and the constituting fragments employing the second-order Møller-Plesset (MP2) methodology (Bernholdt and Harrison, 1996) in combination with Dunning's augmented correlation-consistent quadruple zeta basis set (aug-cc-pVQZ) (see Fig. 3) (Kendall et al., 1992). The resolution of the identity approximation (RI) was used for the MP2 and self-consistent-field (SCF) integrals together with the numerical "chain-of spheres X" (Neese et al., 2009; Kossmann and Neese, 2010) approximation and appropriate fitting basis sets (Weigend, 2002; Weigend, 2006; Weigend, 2008; Weigend et al., 2002) for both the energy and the gradients. The electronic equilibrium dissociation energies (D_e) of the different potential energy minima were subsequently obtained by benchmark Domain-Based Local Pair Natural Orbital Coupled-Cluster Single, Double, and Perturbative Triple [DLPNO-CCSD(T)] (Riplinger et al., 2016; Guo, 2018) single point electronic energy calculations using Dunning's augmented correlation-consistent quintuple zeta basis set (aug-cc-pV5Z) (Kendall et al., 1992) and the RI-JK approximation, on the respective MP2 geometries. The cut-offs were set using the TightPNO option (Liakos et al., 2015). The vibrational ZPE corrected dissociation energies (D_0) were then calculated as the sum of the DLPNO-CCSD(T) electronic dissociation energies and the respective harmonic vibrational ZPE values from the MP2 calculations (see Table 3).

3. Results and discussion

We applied the new methodology to several well-known binary systems of industrial importance. In Fig. 3 we schematically illustrate the pairs of the most stable conformers that we aim to distinguish in this multi-conformational approach. The conformations are arranged according to their association energies or stability, i.e., the higher the conformer is located on the cross-interaction energy axis, the stronger the intermolecular hydrogen bond between the molecules. While this scheme is inspired by the output of spectroscopy and QC research, it does not reflect strictly all the geometric features of these molecular complexes.

Even though the considered binary mixtures have been studied previously with classic CPA modeling (Tsivintzelis et al., 2011; Folas, 2006; Muro-Suñé et al., 2008; Ribeiro et al., 2018; Breil et al., 2011), we consider it a good case study for validating the new approach.

The selected aliphatic alcohol–water complexes have been thoroughly investigated previously with far-IR cluster spectroscopy (Andersen et al., 2015; Andersen et al., 2015). The highly IR-active intermolecular vibrational transitions associated with the class of large-amplitude water librational motion have been detected for the most stable conformations where the water molecule acts as the hydrogen bond donor. These vibrational transitions contribute significantly to the change of vibrational ZPE upon hydrogen bond formation and provide accurate semi-empirical corrections to the purely QC predicted dissociation energies D_0 (Mihrin et al., 2019). The resulting semi-empirical dissociation energies D_0 for the alcohol–water complexes are systematically 0.5 kJ/mol larger than the pure QC results listed in Table 3. However, as minor systematic errors would be introduced in the DI approach whenever semi-empirical ZPE-corrections are not available for both conformations of the alcohol–water complexes, we do not

Table 2
Modeling results and deviations of bubble point pressure (P) and vapor phase mole fraction (y) for water–alcohol binary mixtures.

	T (K)	Association scheme[a]	k_{12}	$m_{(1)}^{A_iB_j}$	$m_{(2)}^{A_iB_j}$	$AARD(P)$, %[b]	$AAD(y)$, %[c]	Exp. data	N[e]
Water–Methanol	298.15–523.15	3B	0	1	0.8997	1.7 (1.8)[d]	0.7 (0.9)[d]	(Kurihara et al., 1995); (Butler et al., 1933); (Griswold and Wong, 1952)	79
Water–Ethanol	298.15–623.15	3B	0	1	0.9120	1.2 (2.0)[d]	0.7 (1.5)[d]	(Kurihara et al., 1995); (Phutela et al., 1979); (Pemberton and Mash, 1978); (Barr-David and Dodge, 1959)	159
Water–Propan-2-ol	298.15–548.15	2B	−0.1120	1	0.9530	1.7 (2.6)[d]	1.5 (1.3)[d]	(Barr-David and Dodge, 1959); (Wu et al., 1988)	106
		3B	−0.0580	1	0.8380	1.8	1.1		
Water–*tert*-Butanol	298.15–348.15	2B	−0.2081	1.0235	0.9109	3.5	2.8	(Brown and Ives, 1962); (Kenttaemaa et al., 1959)	32
		3B	−0.1467	1.0811	0.5720	2.8	2.0		
Water–Phenol	329.45–363.15	2B	−0.0600	0.8691	1.1517	3.5	0.4	(Weller et al., 1963); (Schreinemakers, 1900)	34
		3B	−0.0243	0.7943	1.2203	3.1	0.4		

[a] Association scheme used for alcohols

[b] $AARD(P) = \frac{1}{N}\sum_{i=1}^{N} ABS\left(\frac{P_{\mathrm{exp},i} - P_{\mathrm{calc},i}}{P_{\mathrm{exp},i}}\right) \times 100$

[c] $AAD(y) = \frac{1}{N}\sum_{i=1}^{N} ABS\left(y_{\mathrm{exp},i} - y_{\mathrm{calc},i}\right) \times 100$

[d] The values in brackets are the averaged deviations among all the temperatures in the given range taken from the study (Folas, 2006). The calculations were performed with ECR using one k_{12} for all isothermal data sets.

[e] Number of data points.

consider these empirical corrections in the present contribution. A similar semi-empirical methodology was utilized for the water–acetic acid system (Lopes et al., 2016) and for one of the water–CO_2 conformers (Andersen et al., 2014). The availability of these studies was one of the factors guiding our choice towards the binary systems. Moreover, we aimed to address a representative sample of cross-associating systems covering a substantial range of the intermolecular interactions, even though the systematic evaluation of all possible cross-associations of different nature was not the focus of the present study.

3.1. CPA pure component parameters

The pure component parameters listed in Table 1 were either taken from literature sources or fitted to vapor pressures and liquid densities provided by the DIPPR database.

3.2. Water–Alcohol systems

We selected five water–alcohol (methanol, ethanol, propan-2-ol, *tert*-butanol, and phenol) systems for regression of experimental isothermal VLE data and obtained the correction factors ($m_{(1)}^{A_iB_j}$ and $m_{(2)}^{A_iB_j}$) of CR1-DI listed in Table 2. The parametrization with ECR-DI is presented in Table S1 in the Supplementary Material. The comparison of deviations using the CR1-DI and ECR-DI approaches lead us to the conclusion that the performance of both is quite similar. The water mixtures with methanol and ethanol were modeled without using the binary interaction parameter k_{12}, whereas it was required for the other systems. During the optimization procedure, either both correction factors were regressed, or just one of them, while the other was set to unity. Regressing at least one of the correction factors ($m_{(1)}^{A_iB_j}$ or $m_{(2)}^{A_iB_j}$) is necessary to distinguish the cross-interactions, using the proposed approach. Initially, we regressed a single correction factor ($m_{(1)}^{A_iB_j}$ or $m_{(2)}^{A_iB_j}$) and then the pair of them ($m_{(1)}^{A_iB_j}$ and $m_{(2)}^{A_iB_j}$). If adjusting the second correction factor did not lead to a significant improvement of the pressure and vapor phase mole fraction deviations ($AARD(P)$ and $AAD(y)$), it was set to unity. If using correction factors solely did not yield the desired accuracy for the phase equilibrium properties binary systems, we also adjusted the k_{12} parameter.

We compared our pressure and vapor phase mole fraction deviations with those reported in a previous CPA study (Folas, 2006). For this

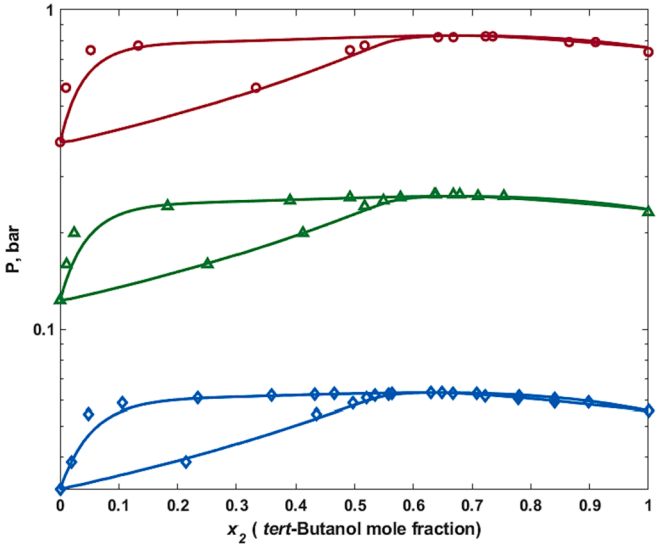

Fig. 4. Water–tert-Butanol (2B) VLE. Symbols (◇– 298.15 K, △– 323.15 K, ○–348.15 K) – experimental data (Brown and Ives, 1962); (Kenttaemaa et al., 1959); lines – CPA calculation using CR1-DI ($k_{12} = -0.2081$, $m_{(1)}^{A_iB_j} = 1.0235$, $m_{(2)}^{A_iB_j} = 0.9109$).

comparison we selected the values related to the modeling using the same association scheme for alcohols as in our calculations and only one value for k_{12} in the entire temperature range for the sake of consistency. There is a slight improvement of deviations for almost all systems compared to the previous results. Even though the same experimental data sources were used for calculations, the difference between our deviations and the referred ones may also be due to the number of data points included. It should be noted that for the water–methanol and the water–ethanol systems, both our results and those reported in (Folas, 2006) are obtained with only one adjustable parameter, whereas for water–propan-2-ol we used one more adjustable parameter.

Sample *P-xy* phase diagrams are presented in Figs. 4–5. These are illustrations of the most challenging cases among the studied systems. Phenol is partially miscible with water and can form azeotropes, which complicates the modeling of the bubble point curves. Nevertheless, the obtained results are in good agreement with the experimental data

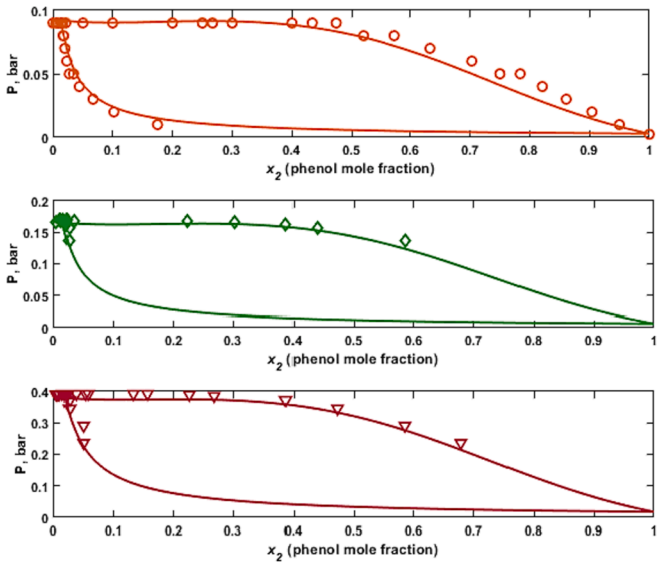

Fig. 5. Water–Phenol (2B) isothermal VLE. Symbols (○ – 317.55 K, ◇ – 329.45 K, ▽ – 348.15 K) experimental data (Weller et al., 1963); (Schreinemakers, 1900); lines – CPA calculations using CR1-DI ($k_{12} = -0.0600$, $m_{(1)}^{A_iB_j} = 0.8691$, $m_{(2)}^{A_iB_j} = 1.1517$).

within the investigated temperature range.

It should be noted that the investigated binary mixtures consist of water and alcohols with compact alkyl or phenyl groups, therefore leading to a limited number of stable conformers. Moreover, the interactions between alkyl or phenyl fragments and the water molecule are significantly weaker than the hydrogen bond, and, therefore, we can approximate the theoretical D_0 association energy of the water–alcohol complex, which includes both dispersive and non-dispersive (electrostatic) interactions, as the cross-association energy $\varepsilon^{A_iB_j}$ used in CPA. The calculated D_0 values are reported in Table 3 and plotted in Fig. 6. The comparison between D_0 and $\varepsilon^{A_iB_j}$ calculated using CR-1 (Table 3) and the pure component parameters listed in Table 1 shows a tendency for $\varepsilon^{A_iB_j}$ to be within the theoretical D_0 -interval involving the two different water–alcohol conformers where the water molecule acts as either a hydrogen bond donor or a hydrogen bond acceptor. This indicates that the $\varepsilon^{A_iB_j}$-value may be considered as an averaged association energy across all conformations.

In general, two association schemes for alcohols (2B and 3B) were used for calculations. However, only the 3B scheme was applied to methanol and ethanol. The association energies for methanol and ethanol with the 2B scheme are 245.9 bar•l/mol (Kontogeorgis et al., 1999) and 215.3 bar•l/mol (Folas et al., 2005), respectively. The corresponding cross-association energies of 206.2 bar•l/mol and 190.9 bar•l/mol, respectively, appear to be an overestimation in comparison with the theoretical D_0 values for these cross-interactions. Therefore, we excluded the 2B scheme from our consideration in the abovementioned cases and proceeded with the association schemes listed in Tables 2–3 that are consistent with the theoretical input. Of the numerous conformers coexisting in the mixture, the most stable ones are water (HB donor)–alcohol (HB acceptor) and water (HB acceptor)–alcohol (HB donor), which are further denoted as conformer (1) and conformer (2), respectively. Conformer (1) (red symbols in Fig. 6) has a higher association energy than conformation (2) (blue symbols in Fig. 6) for the series of aliphatic alcohols, whereas the two conformations of the water–phenol complex follow the opposite trend.

We used the obtained correction factors ($m_{(1)}^{A_iB_j}$ and $m_{(2)}^{A_iB_j}$) of CR1-DI to calculate the association energies $\varepsilon^{A_iB_j}$ of the two different conformers. These energies are listed in Table 3 and illustrated in Fig. 6.

As can be seen in Fig. 6, a quite satisfactory agreement between D_0 and $\varepsilon_{(1)}^{A_iB_j}$, $\varepsilon_{(2)}^{A_iB_j}$ is observed for the water–methanol and water–ethanol systems, although in the latter case, conformer (1) fails to follow the trend of stabilization with the increasing chain length due to the inductive effect. This can be explained by the same inconsistency for the pure component association energies of water, methanol, and ethanol used in the fitting procedure of binary mixtures (Table 1). At the molecular level, a longer hydrocarbon chain increases the electron density on the O-atom of the hydroxy group due to the inductive effect, thereby strengthening the hydrogen bond (Mihrin et al., 2022). Therefore, it is expected that the values of self-association energy follow the trend: ethanol > methanol > water. Analogously, the association energy for the ethanol–water complex is expected to be higher than that for the methanol–water complex (Nedić et al., 2011; Andersen et al., 2015; Andersen et al., 2015).

Aqueous mixtures of propan-2-ol or *tert*-butanol were modeled with both the 2B and 3B association schemes. In the case of propan-2-ol, discrepancies between D_0 and $\varepsilon_{(1)}^{A_iB_j}$, $\varepsilon_{(2)}^{A_iB_j}$ are observed for both schemes. However, the ratio R_ε between the two conformers for 3B matches the ratio R_{D_0} quite well, while R_ε for the 2B scheme seems to be underestimated in comparison with R_{D_0}. Both cross-association energies

Table 3
Comparison between the theoretical ZPE-corrected association energies (D_0) and cross-association energies (all values are in bar•l/mol) calculated with CPA.

		Conformer (1)		Conformer (2)				
	$\varepsilon^{A_iB_j}$ [a]	$D_{0(1)}$	$\varepsilon_{(1)}^{A_iB_j}$ [b]	$D_{0(2)}$	$\varepsilon_{(2)}^{A_iB_j}$ [b]	R_{D_0} [c]	R_ε [d]	Association scheme [e]
Water–Methanol	163.63	159	163.63	144	147.21	1.104	1.112	3B
Water–Ethanol	158.28	173	158.28	148	144.35	1.169	1.097	3B
Water–Propan-2-ol	188.28	188	188.28	149	179.39	1.262	1.050	2B
	168.78		168.78		141.37		1.194	3B
Water–*tert*-Butanol	199.78	195	204.47	155	181.98	1.258	1.124	2B
	183.28		198.14		104.84		1.890	3B
Water–Phenol	170.72	132	148.37	218	196.62	0.606	0.755	2B
	161.79		128.51		197.43		0.651	3B

[a] Cross-association energies calculated with CR-1.
[b] Cross-association energies obtained with CR1-DI.
[c] $R_{D_0} = \frac{D_{0(1)}}{D_{0(2)}}$.
[d] $R_\varepsilon = \frac{\varepsilon_{(1)}^{A_iB_j}}{\varepsilon_{(2)}^{A_iB_j}}$.
[e] The association scheme used for alcohol.

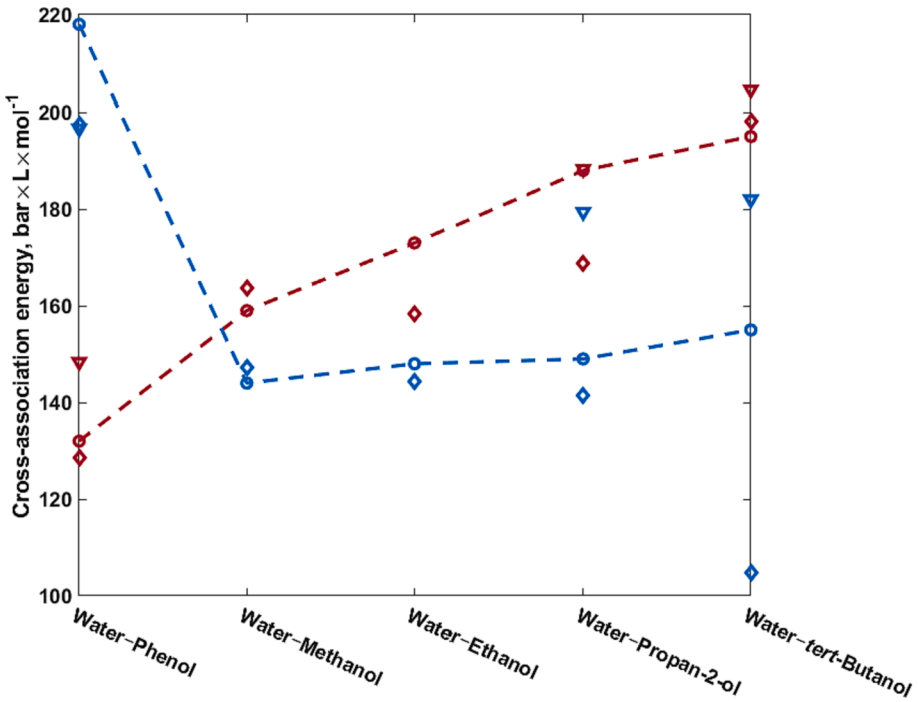

Fig. 6. Comparison between the theoretical ZPE-corrected association energies D_0 (– ⊖ – conformer (1), – ⊖ – conformer (2)) and, $\varepsilon_{(1)}^{A_iB_j}$, $\varepsilon_{(2)}^{A_iB_j}$ regressed with CPA using CR1-DI (the association energies $\varepsilon^{A_iB_j}$ of the two different conformers are listed in Table 3). Alcohols were modeled with two association schemes: 2B (▽- conformer (1), ▽- conformer (2)) and 3B (◇- conformer (1), ◇- conformer (2)).

and their ratios regarding the water–*tert*-butanol system calculated with the 3B scheme highly deviate from D_0 and R_{D_0}, whereas the results obtained with the 2B scheme are in better agreement with the theoretical values. This observation may be explained by the growing influence of steric hindrance with the increase of alkyl group size, which prevents the formation of two hydrogen bonds with the two accessible lone pairs of electrons on the O-atom. This is especially the case for *tert*-butanol, which is composed of three flexible methyl groups that might hinder the hydroxy group. Notably, the modeling results for the water–phenol system show a reasonably good agreement with D_0, especially using the 3B scheme. Presumably, the rigid phenyl group does not significantly sterically hinder the oxygen atom and, moreover, increases its electron density due to inductive and resonance effects. In principle, these reflections based on the molecular structure and microscopic association energies should guide an optimal selection of the association scheme.

3.3. Water–Acetic acid

The phase equilibrium of water–acetic acid has been widely investigated both experimentally and theoretically due to its high industrial importance, especially for distillation processes. Previous studies (Breil et al., 2011; Muro-Suñé et al., 2008; Kontogeorgis et al., 2006) have reported challenges in modeling the VLE of this system using CPA and have proposed combining CPA with Huron-Vidal mixing rule. Even though this approach provides an accurate description, it increases computational complexity and the number of adjustable parameters compared to the classic CPA modeling. To evaluate the performance of the new cross-interactions framework, we applied it to the modeling of water–acetic acid VLE. Although the considered approach also leads to an increased number of adjustable parameters, it does not increase computational complexity.

It has been shown previously (Wolbach and Sandler, 1997; Derawi et al., 2004; Tsonopoulos and Prausnitz, 1970) that acetic acid strongly dimerizes in the vapor phase by doubly strongly cooperative intermolecular hydrogen bonds, which promotes the implementation of the 1A association scheme (one bipolar association site per molecule of acetic acid). Despite the high self-association tendency of acetic acid, the studies of its binary complexes with water show that stable cyclic mixed associates (Fig. 3) are formed (Lopes et al., 2016), which highlights the problem with utilizing the 1A scheme for acetic acid. Nevertheless, the 1A scheme has been successfully used in the case of other mixtures, both polar and non-polar (Muro-Suñé et al., 2008; Folas et al., 2005; Derawi et al., 2004; Kontogeorgis et al., 2006; Perakis et al., 2007) and was therefore also considered in this study. In addition, we investigated the performance of the 2B association scheme for acetic acid. To determine the correction factors of CR1-DI and ECR-DI as well as the binary interaction coefficient k_{12}, we regressed the isothermal VLE experimental data in a wide range of temperatures (353.15 – 509.2 K). The obtained binary parameters and deviations of calculations from experiment are presented in Table 4. To obtain the correction factors $m_{(1)}^{A_iB_j}$ and $m_{(2)}^{A_iB_j}$, we used reported association energies (Lopes et al., 2016) as a guide for initial estimates: 116 bar•l/mol for water (HB donor)–acetic acid (HB acceptor) and 210 bar•l/mol for water (HB acceptor)–acetic acid (HB donor). We used these approximations for calculations with both schemes, although the physical picture of intermolecular interactions is better captured by the 2B scheme instead of the 1A scheme. It should be noted that the corresponding conformations are not the most stable ones, but they are appropriate for the localized site-to-site energy approximations due to the non-cyclic structure and eliminated impact of dispersion forces from the non-hydrogen bond interactions. However, the most stable cyclic conformer formed through two interactions between acetic acid and water cannot be introduced explicitly with either of the association schemes. Consequently, cross-association energies recalculated from the correction factors $m_{(1)}^{A_iB_j}$ and $m_{(2)}^{A_iB_j}$ modeled with the 2B scheme for acetic acid are more consistent with theoretical guidelines than similar calculations performed with 1A.

In Figs. 7–8 we compared the calculated and experimental data on both isothermal and isobaric VLE. According to some *P-xy* data (Freeman and Wilson, 1985), a pinch point is observed in the water-rich

Table 4
Binary parameters, cross-association energies (all values are in bar•l/mol), and deviations for the water–acetic acid system.

Association scheme [a]	k_{12}	$m_{(1)}^{A_iB_j}$	$m_{(2)}^{A_iB_j}$	$\varepsilon_{(1)}^{A_iB_j}$	$\varepsilon_{(2)}^{A_iB_j}$	$AARD(P)$[b], %	$AAD(y)$[b], %
1A	−0.1993	0.4663	1.1215	132.84	319.50	1.8	1.6
2B	−0.2182	0.8218	1.1021	145.75	195.45	1.7	1.6

[a] The association scheme used for acetic acid.
[b] Number of data points = 73.

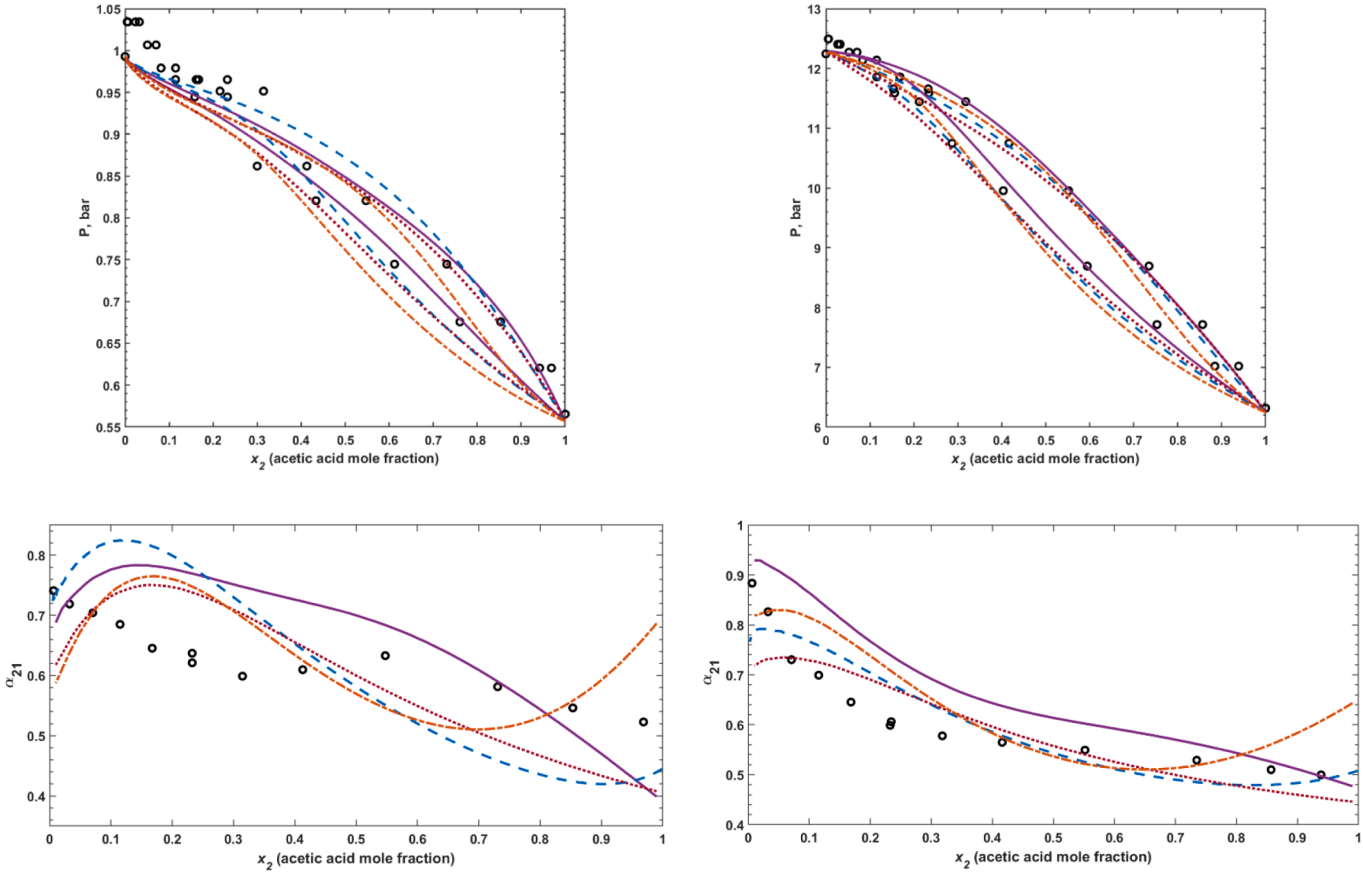

Fig. 7. P-*xy* phase diagrams of water–acetic acid at 372.8 K (top left) and 462.1 K (top right) and corresponding relative volatilities ($\alpha_{12} = \frac{y_2}{x_2} \times \frac{x_1}{y_1}$) plots at 372.8 K (bottom left) and 462.1 K (bottom right). Experimental data (Freeman and Wilson, 1985) indicated with symbols (o), corresponding lines are the CPA calculations with different association schemes used for acetic acid (1A or 2B) and combining rules (CR1-DI or near ECR). Solid lines: CR1-DI, 1A (k_{12} = -0.1993, $m_{(1)}^{A_iB_j}$ = 0.4663, $m_{(2)}^{A_iB_j}$ = 1.1215). Dashed lines: CR1-DI, 2B (k_{12} = -0.2182, $m_{(1)}^{A_iB_j}$ = 0.8218, $m_{(2)}^{A_iB_j}$ = 1.1021). Dotted lines: near ECR, 2B (k_{12} = − 0.2271) (Ribeiro et al., 2018). Dash-dotted lines: near ECR, 1A ($k_{12,372.8K}$ = − 0.2468, $k_{12,462.1K}$ = − 0.2410) (Ribeiro et al., 2018).

region, although some *T-xy* data (Ito and Yoshida, 1963) do not seem to indicate the same phenomenon. The pressure and vapor mole fraction deviations (*AARD(P), AAD(y)*) are within a reasonable percentage. In general, modeling with both association schemes provides good results, although the demonstrated examples (Figs. 7–8) exhibit slightly inferior performance of the 2B scheme in those cases. Fig. 7 also demonstrates the comparison between our approach and CPA modeling using ECR (Ribeiro et al., 2018) with one k_{12}-parameter, which is in one case temperature dependent. It should be noted that our approach requires three adjustable parameters.

The dissociation of acetic acid in water should in principle be included in the modeling. Neither the current study nor most of the previous modeling studies using CPA include the dissociation equilibrium explicitly. Besides, the 1A scheme is an oversimplification of the actual association in the water-acetic acid system. Therefore, this system may not be the most adequate system to evaluate our proposed approach. Nevertheless, the system is industrially important, and its modeling with the new approach is valuable for practical applications.

3.4. Water–CO_2

The water–CO_2 system plays a central role in geological CO_2 storage that is used to reduce CO_2 emissions. Moreover, the binary system forms weakly bound complexes in the mixture, whereas CO_2 is generally assumed to be non-associating in its pure form. Therefore, the binary system presents an interesting case in terms of validating the new approach. The investigation of this system might broaden the application of the DI approach to a variety of intermolecular interactions.

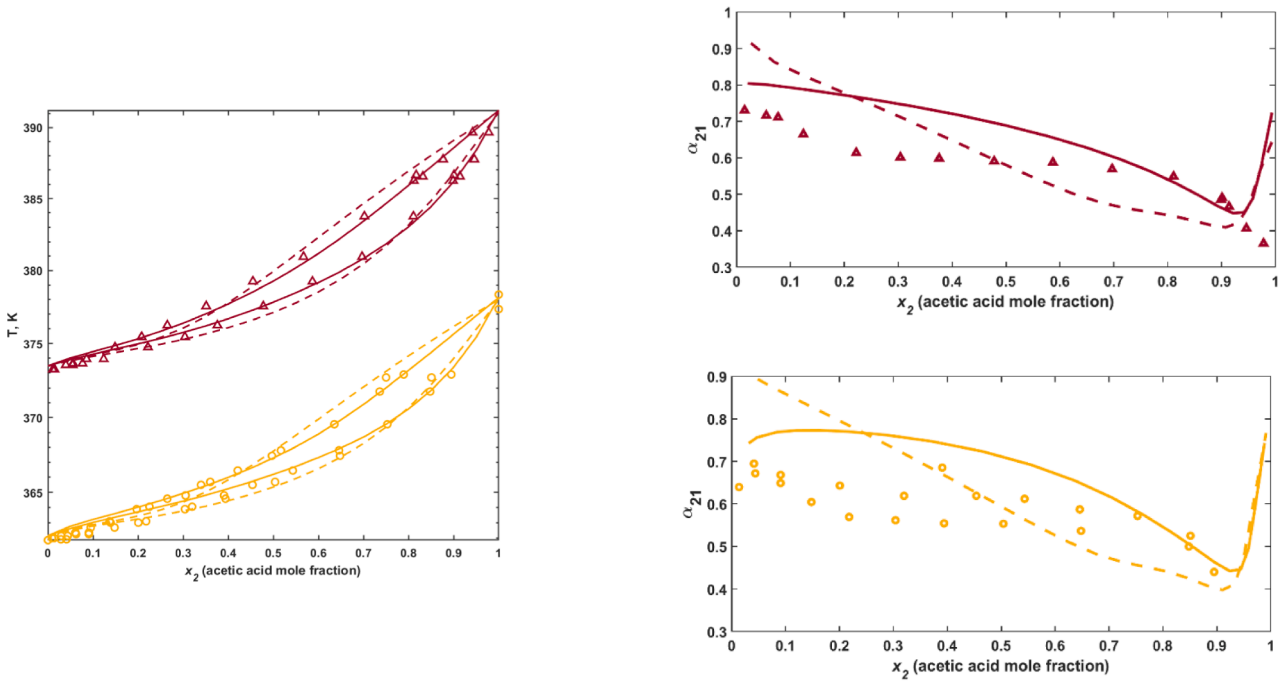

Fig. 8. T-*xy* phase diagrams (left) and relative volatilities ($\alpha_{12} = \frac{y_2}{x_2} \times \frac{x_1}{y_1}$) (right) of water–acetic acid: experimental data (Ito and Yoshida, 1963) indicated with symbols (○- 0.6666 bar, △– 1.013 bar), corresponding lines are the CPA calculations with different association schemes used for acetic acid (solid lines – CR1-DI, 1A: k_{12} = -0.1993, $m^{A_iB_j}_{(1)}$ = 0.4663, $m^{A_iB_j}_{(2)}$ = 1.1215, dashed lines – CR1-DI, 2B: k_{12} = -0.2182, $m^{A_iB_j}_{(1)}$ = 0.8218, $m^{A_iB_j}_{(2)}$ = 1.1021).

It has been reported previously that the water–CO_2 complex forms two different conformations (Danten et al., 2005; Sadlej and Mazurek, 1995). The first one (conformer (1)) is formed with a C-atom of CO_2 and an O-atom of water. This complex is mostly kept together by dispersion forces and an electrostatic dipole (water)–quadrupole (CO_2) interaction. In this case, carbon corresponds to the positive site and oxygen to the negative site. The formation of this complex has been confirmed by various theoretical and experimental studies, and the association energies vary from 83 to 142 bar•l/mol (Andersen et al., 2014; Danten et al., 2005; Sadlej and Mazurek, 1995; Wormald et al., 1983). Conformer (2) is formed by the electrostatic interaction between an oxygen atom of CO_2 and a hydrogen atom of water. The association energy of this conformation is in the range of 41.84–50 bar•l/mol (Danten et al., 2005; Sadlej and Mazurek, 1995) and it appears to be less stable than conformer (1). The CO_2 self-association in thermodynamic modeling is generally neglected, although it has been investigated in some theoretical studies, for instance, interaction energies between 28 and 44 bar•l/mol were reported in ref. (Tsuzuki et al., 1996).

Table 5

CPA individual (ε^{CO_2}) and binary (fixed ($\varepsilon^{A_iB_j}_{(1)}$,$\varepsilon^{A_iB_j}_{(2)}$) and regressed ($k_{12}$,$\beta^{A_iB_j}$)[a]) parameters using CR1-DI for the water–CO_2 system.

ε^{CO_2} [b]	Regressed k_{12}	$\beta^{A_iB_j}$	Fixed $\varepsilon^{A_iB_j}_{(1)}$ [b]	$\varepsilon^{A_iB_j}_{(2)}$ [b]	$AAD(x)$[c]	$AAD(y)$[d]
0	0.08322	0.08276	85.6	36.7	15.3	20.2
	0.10777	0.01559	142	36.7	9.4	11.5
46.2	0.05340	0.08148	85.6	36.7	15.0	22.3
	0.08351	0.01641	142	36.7	9.5	10.2
78.12	−0.08424	0.04377	85.6	36.7	17.5	39.0
	0.00542	0.02077	142	36.7	14.8	7.5

[a] Experimental data for the fitting are taken from refs. (Wiebe and Gaddy, 1940; King et al., 1992; Valtz et al., 2004; Gillespie, 1982; Wiebe and Gaddy, 1941; Wiebe and Gaddy, 1939; Bamberger et al., 2000). Number of data points = 207.

[b] All association energy values are in bar•l/mol.

[c] $AAD(x) = \frac{1}{N}\sum_{i=1}^{N} ABS(x_{\exp,i} - x_{calc,i}) \times 100.$

[d] $AAD(y) = \frac{1}{N}\sum_{i=1}^{N} ABS\left(y_{\exp,i} - y_{calc,i}\right) \times 100.$

It should be noted that some of the interaction energies listed above were calculated with less accurate techniques than the one used for the QC calculations in the present study. Therefore, for the sake of consistency we calculated the D_0-values related to the conformations of the weakly bound water–CO_2 van der Waals complex and the CO_2 dimer using the DLPNO-CCSD(T) approach without the spectroscopic ZPE-corrections. The obtained D_0 for conformers (1) and (2) are 85.6 and 36.7 bar•l/mol, respectively. The D_0-value for conformer (1) has also been determined using semi-empirical ZPE-correction resulting in 86.8 bar•l/mol (Andersen et al., 2014), which differs from the purely theoretical value insignificantly. The benchmark value at the same level of theory for the CO_2 dimer is 46.2 bar•l/mol. These results were further used in the fitting procedure using the DI approach.

The DI approach allows one to account for the second type of interaction in the calculations explicitly. Following the methodology of Tsivintzelis et al. (Tsivintzelis et al., 2011), the association energy of the most stable conformation was fixed to 142 bar•l/mol (Wormald et al., 1983), while k_{12} and $\beta^{A_iB_j}$ were fitted to experimental data. In addition, the association energy of the less stable conformer was set to 36.7 bar•l/mol without further variation. Therefore, our modeling approach involves the same number of adjustable parameters as the work of Tsivintzelis et al. (Tsivintzelis et al., 2011). We suspect that 142 bar•l/mol might be an overestimation of the described interaction strength. However, replacing this value with the lower DLPNO-CCSD(T) benchmark value of this study (85.6 bar•l/mol) will lead to a greater discrepancy with the experimental thermodynamic data (Table 5 and Fig. 9). It is worth noting that the SAFT theory was originally developed for localized site-to-site interactions; however, the water–CO_2 system does not entirely fulfill this requirement and we might expect some deviations from the theoretical benchmark value while modeling this system.

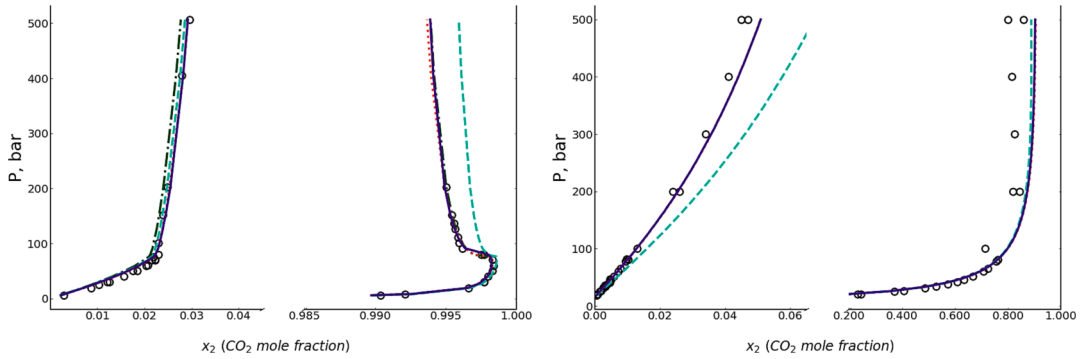

Fig. 9. VLE of water–CO_2 at 308.2 K on the left and at 473.15 K on the right. Experimental data (Wiebe and Gaddy, 1940; King et al., 1992; Valtz et al., 2004; Zawisza and Malesinska, 1981; Toedheide and Franck, 1963; Müller et al., 1988; Takenouchi and Kennedy, 1964) are marked with symbols and the corresponding lines are the calculations with CPA. Dash-dotted lines: solvation, accounting for one complex ($\varepsilon_{(1)}^{A_iB_j}$=142 bar•l/mol) (Tsivintzelis et al., 2011). Dotted lines: solvation, accounting for two types of complexes ($\varepsilon_{(1)}^{A_iB_j}$=142 bar•l/mol, $\varepsilon_{(2)}^{A_iB_j}$= 36.7 bar•l/mol). Dashed lines: solvation, accounting for two types of complexes ($\varepsilon_{(1)}^{A_iB_j}$=85.6 bar•l/mol, $\varepsilon_{(2)}^{A_iB_j}$= 36.7 bar•l/mol). Solid lines: self-association (ε^{CO_2}=46.2 bar•l/mol), two types of complexes ($\varepsilon_{(1)}^{A_iB_j}$=142 bar•l/mol, $\varepsilon_{(2)}^{A_iB_j}$= 36.7 bar•l/mol).

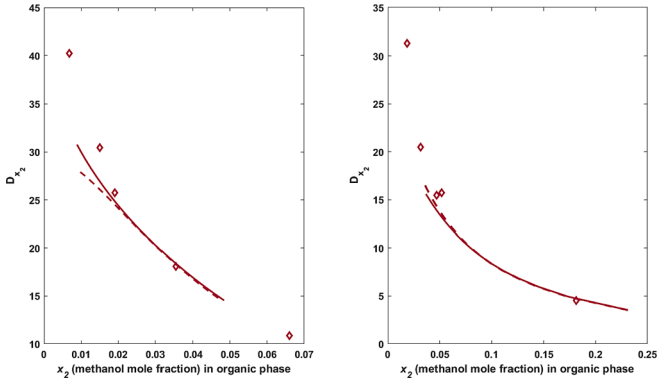

Fig. 10. Water (1)–methanol (2)–propane (3) LLE at 293.15 K and 9 bar on the left (experimental data – (Noda et al., 1975); water (1)–methanol (2) –hexane (3) LLE at 293.15 K and 1 bar on the right (experimental data – (Kogan et al., 1956). Distribution of methanol (D_{x_2}) between aqueous (x_2^{aq}) and organic (x_2^{org}) phases is calculated with the equation: $D_{x_2} = \frac{x_2^{aq}}{x_2^{org}}$. Solid lines – calculation with CR1-DI for water–methanol (3B): $k_{12} = 0$, $m_{(1)}^{A_iB_j} = 0$, $m_{(2)}^{A_iB_j} = 0.8997$, dashed lines – calculation with ECR for water–methanol (3B): $k_{12} = 0.035$ (Folas, 2006). The parameters for other binary systems are the same for both cases. Water–propane: $k_{13} = 0$; water–hexane: $k_{13} = 0$; methanol–propane: $k_{23} = -0.029$ (Folas, 2006); methanol–hexane: $k_{23} = -0.036$ (Folas, 2006).

The generated results presented in Table 5 cover six cases that differ by the self-association energy of CO_2 and cross-association energy of the conformer (1). Fig. 9 demonstrates good agreement between the modeling and experimental data at 308.2 K and 473.15 K, respectively, except for the calculations with $\varepsilon_{(1)}^{A_iB_j}$ = 85.6 bar•l/mol.

We demonstrate with this example that the DI approach can not only be applied to hydrogen-bonded dimers but also to molecular complexes involving weaker van der Waals interactions.

3.5. Phase equilibrium of ternary systems

The results obtained for binary cross-associating systems with CR1-DI were used for the phase equilibrium calculations of several ternary systems. Most of the selected ternary systems contain water, alcohol, and hydrocarbons. Even though these systems have previously been modeled with CPA, some issues have been reported while using the 3B scheme for methanol (Kontogeorgis et al., 2006). Therefore, we aim to investigate if the novel approach could lead to any improvement in problematic cases. In addition, we investigated the water–acetic acid–CO_2 system that contains two binary systems modeled using our new approach.

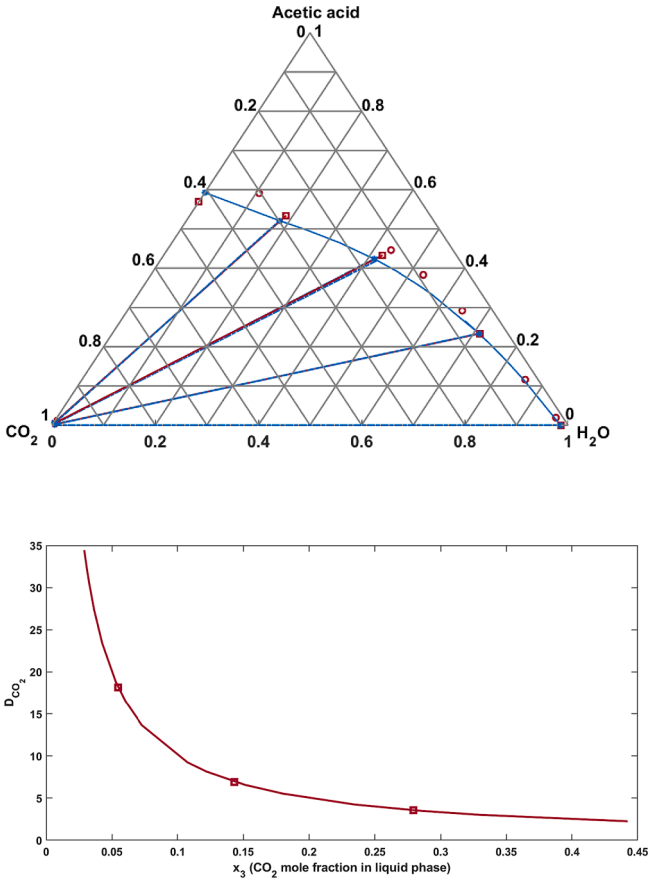

Fig. 11. Ternary VLE of water (1)–acetic acid (2)–CO_2 (3) at 333 K and 61 bar. Experimental data ■ – (Bamberger et al., 2004), ● – (Panagiotopoulos et al., 1988), ✱ – prediction with CPA. Binary systems parameters: water–acetic acid (1A): $k_{12} = -0.1993$, $m_{(1)}^{A_iB_j} = 0.4663$, $m_{(2)}^{A_iB_j} = 1.1215$; water–$CO_2$ (no self-association): $k_{13} = 0.10777$, $\beta^{A_iB_j} = 0.01559$, $\varepsilon_{(1)}^{A_iB_j} = 142$ bar•l/mol, $\varepsilon_{(2)}^{A_iB_j} = 36.7$ bar•l/mol; acetic acid–CO_2: $k_{23} = 0$. $D_{CO_2} = \frac{y_{CO_2}}{x_{CO_2}}$.

In Fig. 10 we compared calculations using CR1-DI and ECR (Folas, 2006) for water–methanol–propane/hexane systems. Clearly the performance of the two considered approaches is similar and no significant

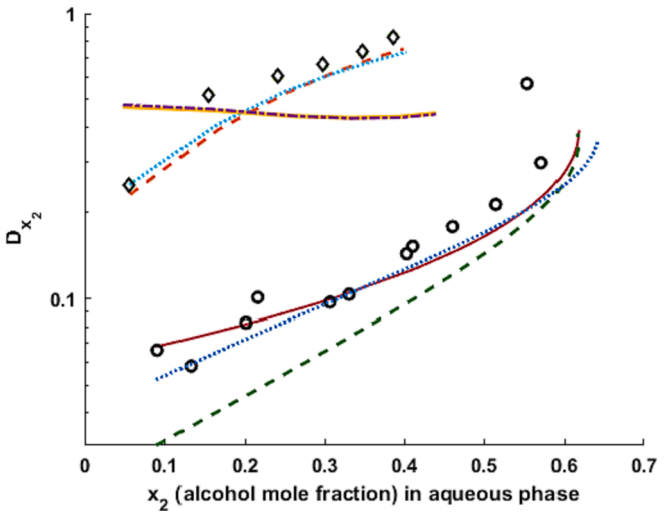

Fig. 12. Ternary LLE of water (1)–methanol (2)–benzene (3) at 303.15 K and 1.013 bar: experimental data (Gramajo de Doz et al., 2001) (○); water (1)–ethanol (2)–benzene (3) at 308.15 K and 1.013 bar: experimental data (Sørensen, Pa. 1980.) (◇). Distribution of methanol (D_{x_2}) between aqueous (x_2^{aq}) and organic (x_2^{aq}) phases is calculated with the equation: $D_{x_2} = \frac{x_2^{aq}}{x_2^{org}}$. Corresponding lines – predictions with CPA. Solid lines – calculations with CR1-DI (water–methanol (3B): $k_{12} = 0$, $m_{(1)}^{A_iB_j} = 0$, $m_{(2)}^{A_iB_j} = 0.8997$; water–ethanol (3B): $k_{12} = 0$, $m_{(1)}^{A_iB_j} = 0$, $m_{(2)}^{A_iB_j} = 0.9116$; methanol (3B)–benzene (no solvation) $k_{23} = -0.012043$; ethanol (3B)–benzene (no solvation) $k_{23} = 0.01408$; water–benzene (solvation (Folas et al., 2006): $k_{13} = 0.0355$, $\beta^{A_iB_j} = 0.079$). Dashed lines – calculations with ECR (Folas et al., 2006) (water – methanol (2B): $k_{12} = -0.09$; water–ethanol (2B): $k_{12} = -0.11$; methanol (2B)–benzene: $k_{13} = 0.006$, ethanol (2B)–benzene: $k_{13} = 0.02$; water–benzene (solvation): $k_{13} = 0.0355$, $\beta^{A_iB_j} = 0.079$). Dotted lines–calculations with ECR (Folas et al., 2006) (water–methanol (2B): $k_{12} = -0.09$; water–ethanol (2B): $k_{12} = -0.11$; methanol (2B)–benzene (solvation): $k_{13} = 0.02$, $\beta^{A_iB_j} = 0.01$; ethanol (2B)–benzene (solvation): $k_{13} = 0.022$, $\beta^{A_iB_j} = 0.002$; water–benzene (solvation): $k_{13} = 0.0355$, $\beta^{A_iB_j} = 0.079$). Dash-dotted lines – calculations with ECR (water–ethanol (3B): $k_{12} = 0$ (Folas, 2006); ethanol (3B)–benzene (no solvation): $k_{23} = 0.01408$; water–benzene (solvation (Folas et al., 2006): $k_{13} = 0.0355$, $\beta^{A_iB_j} = 0.079$).

improvement is observed.

To model the ternary VLE of the water–acetic acid–CO_2 system we used the 1A association scheme for acetic acid and did not account for any solvation in the case of CO_2. It can be seen in Fig. 11 that the calculation results match experimental data very well.

The LLE for the ternary water–methanol–benzene and water–ethanol–benzene systems were calculated with the parameters for water–alcohol listed in Table 2. We used the solvation approach proposed in ref. (Folas et al., 2006) for the binary water–benzene system; however, solvation was not considered in the case of the alcohol–benzene system. Fig. 12 shows a fair agreement between the experimental and calculated data for the water–methanol–benzene system; however, discrepancies significantly increase for the water–ethanol–benzene system. Our results for the methanol system are slightly better than those presented previously (Folas et al., 2006), but significantly inferior for the mixtures with ethanol (Fig. 12). Accounting for solvation between alcohol and benzene will not improve the predictions in both cases. We also performed calculations for the water–ethanol–benzene system, using the 3B association scheme for ethanol and ECR for water–ethanol ($k_{12} = 0$), and observed the same performance as with CR1-DI approach. We suspect there might be some issues with using the 3B association scheme for ethanol while modeling this particular system regardless of the cross-association approach. This speculation is supported by the observed inconsistency of the ethanol association energy with the 3B scheme, which may affect the results as well.

4. Conclusions

In the present work we introduced a framework that allows us to distinguish different molecular conformations. Currently the conventional combining rules used in EoSs only account for one conformer, while our proposed approach allows one to account for a pair of conformers present in a binary mixture. The proposed approach is based on CPA and relies on the QC calculations of intermolecular association energies. The major advantage of the proposed methodology is the consideration of the asymmetry of hydrogen bonding between different species, which was either partly overlooked in previous SAFT-type models or was not justified and connected with intermolecular interactions on a microscopic level. The proposed approach builds a bridge between the SAFT theory and microscopic quantum chemical studies. The introduced cross-association framework involves the modification of the most common combining rules ECR and CR-1 by introducing two correction factors that mark the difference between these conformations.

This approach was used to model the binary VLE of aqueous mixtures with alcohols (methanol, ethanol, propan-2-ol, *tert*-butanol, and phenol), acetic acid, and CO_2. Water–alcohol systems were regressed with both the CR1-DI and ECR-DI combining rules, and it was subsequently shown that there is not a substantial difference in their performance. Methanol and ethanol were modeled only with the 3B scheme, while other alcohols were modeled with both the 2B and 3B schemes. We observed a quite satisfactory agreement between the cross-association energies obtained by fitting thermodynamic experimental data using the new approach and the microscopic values (D_0) from QC predictions.

We achieved improvements in the modeling of water–acetic acid VLE, particularly using the 1A association scheme applied to acetic acid. However, both the 1A and 2B schemes led to a good agreement with the experimental data.

Apart from the mixtures with strong hydrogen bonding between the associating compounds, the solubility in the water–CO_2 system was investigated. Two conformations of the weakly bound water–CO_2 van der Waals complex were considered, and different pairs of interaction energies were evaluated. We treated CO_2 as both a cross-associating and a non-self-associating molecule.

Based on the new results for the binary systems, ternary LLE of water–alcohol–hydrocarbon mixtures and VLE of the water–acetic acid–CO_2 system were calculated. The predictions for water–alcohol–hydrocarbon mixtures are in qualitative agreement with experimental data, although further improvements are still required. For the ternary water–acetic acid–CO_2 system, our calculation reproduced experimental VLE very well.

Declaration of Competing Interest

The authors declare that they have no known competing financial interests or personal relationships that could have appeared to influence the work reported in this paper.

Data availability

No data was used for the research described in the article.

Appendix A. Supplementary data

Supplementary data to this article can be found online at https://doi.org/10.1016/j.ces.2023.119404.

References

Andersen, J., Heimdal, J., Wugt Larsen, R., 2015. Spectroscopic identification of ethanol-water conformers by large-amplitude hydrogen bond librational modes. J. Chem. Phys. 143 (22) https://doi.org/10.1063/1.4937482.

Andersen, J., Heimdal, J., Mahler, D.W., Nelander, B., Wugt Larsen, R., 2014. Communication: THz absorption spectrum of the CO2-H2O complex: observation and assignment of intermolecular van der Waals vibrations. J. Chem. Phys. 140 (9), pp. https://doi.org/10.1063/1.4867901.

Andersen, J., Heimdal, J., Wugt Larsen, R., 2015. The influence of large-amplitude librational motion on the hydrogen bond energy for alcohol-water complexes. PCCP 17 (37), 23761–23769. https://doi.org/10.1039/c5cp04321b.

Avlund, A.S., Kontogeorgis, G.M., Chapman, W.G., 2011. Intramolecular association within the SAFT framework. Mol. Phys. 109 (14), 1759–1769. https://doi.org/10.1080/00268976.2011.589990.

Bamberger, A., Sieder, G., Maurer, G., 2000. High-pressure (vapor+liquid) equilibrium in binary mixtures of (carbon dioxide+water or acetic acid) at temperatures from 313 to 353 K. J. Supercrit. Fluids 17 (2), 97–110. https://doi.org/10.1016/S0896-8446(99)00054-6.

Bamberger, A., Sieder, G., Maurer, G., 2004. High-pressure phase equilibrium of the ternary system carbon dioxide + water + acetic acid at temperatures from 313 to 353 K. J. Supercrit. Fluids 32 (1–3), 15–25. https://doi.org/10.1016/j.supflu.2003.12.014.

Barr-David, F., Dodge, B.F., 1959. Vapor-liquid equilibrium at high pressures. the systems ethanol-water and 2-propanol-water. J. Chem. Eng. Data 4 (2), 107–121. https://doi.org/10.1021/je60002a003.

Bernholdt, D.E., Harrison, R.J., 1996. Large-scale correlated electronic structure calculations: the RI-MP2 method on parallel computers. Chem. Phys. Lett. 250 (5–6), 477–484. https://doi.org/10.1016/0009-2614(96)00054-1.

Breil, M.P., Kontogeorgis, G.M., Behrens, P.K., Michelsen, M.L., 2011. Modeling of the thermodynamics of the acetic acid-water mixture using the cubic-plus-association equation of state. Ind. Eng. Chem. Res. 50 (9), 5795–5805. https://doi.org/10.1021/ie102105r.

Brown, A.C., Ives, D.J.G., 1962. 311. The t-butyl alcohol–water system. J. Chem. Soc. 1608–1619. https://doi.org/10.1039/JR9620001608.

Butler, J.A.V., Thomson, D.W., Maclennan, W.H., 1933. 173. The free energy of the normal aliphatic alcohols in aqueous solution. Part I. The partial vapour pressures of aqueous solutions of methyl, n-propyl, and n-butyl alcohols. Part II. The solubilities of some normal aliphatic alcohols in water. Part III. J. Chem. Soc. 674. https://doi.org/10.1039/jr9330000674.

Chapman, W.G., Jackson, G., Gubbins, K.E., 1988. Phase equilibria of associating fluids chain molecules with multiple bonding sites. Mol. Phys. 65 (5), 1057–1079. https://doi.org/10.1080/00268978800101601.

Chapman, W.G., Gubbins, K.E., Jackson, G., Radosz, M., 1989. SAFT: Equation-of-state solution model for associating fluids. Fluid Phase Equilib. 52, 31–38. https://doi.org/10.1016/0378-3812(89)80308-5.

Chapman, W.G., Gubbins, K.E., Jackson, G., Radosz, M., 1990. New reference equation of state for associating liquids. Ind. Eng. Chem. Res. 29 (8), 1709–1721. https://doi.org/10.1021/ie00104a021.

Danten, Y., Tassaing, T., Besnard, M., 2005. Ab initio investigation of vibrational spectra of water-(CO2)n complexes (n = 1, 2). Chem. A Eur. J. 109 (14), 3250–3256. https://doi.org/10.1021/jp0503819.

Derawi, S.O., Zeuthen, J., Michelsen, M.L., Stenby, E.H., Kontogeorgis, G.M., 2004. Application of the CPA equation of state to organic acids. Fluid Phase Equilib. 225 (1–2), 107–113. https://doi.org/10.1016/j.fluid.2004.08.021.

Dufal, S., et al., 2014. Prediction of thermodynamic properties and phase behavior of fluids and mixtures with the SAFT-γ mie group-contribution equation of state. J. Chem. Eng. Data 59 (10), 3272–3288. https://doi.org/10.1021/je500248h.

Folas, G.K., 2006. Modeling of complex mixtures containing hydrogen bonding molecules. PhD thesis. Technical University of Denmark.

Folas, G.K., Derawi, S.O., Michelsen, M.L., Stenby, E.H., Kontogeorgis, G.M., 2005. Recent applications of the cubic-plus-association (CPA) equation of state to industrially important systems. Fluid Phase Equilib. 228–229 (1), 121–126. https://doi.org/10.1016/j.fluid.2004.08.013.

Folas, G.K., Gabrielsen, J., Michelsen, M.L., Stenby, E.H., Kontogeorgis, G.M., 2005. Application of the cubic-plus-association (cpa) equation of state to cross-associating systems. Ind. Eng. Chem. Res. 44 (10), 3823–3833. https://doi.org/10.1021/ie048832j.

Folas, G.K., Kontogeorgis, G.M., Michelsen, M.L., Stenby, E.H., 2006. Application of the cubic-plus-association (cpa) equation of state to complex mixtures with aromatic hydrocarbons. Ind. Eng. Chem. Res. 45 (4), 1527–1538. https://doi.org/10.1021/ie050976q.

Freeman, J.R., Wilson, G.M., 1985. High Temperature Vapor-Liquid Equilibrium Measurements on Acetic Acid/Water Mixtures. AlChE Symp. Ser. 81 (244), 14–25.

Gillespie, G.M., Wilson, P.C., 1982. Gas Processor Association, Research Report RR48. Tulsa, OK.

Gramajo de Doz, M.B., Bonatti, C.M., Barnes, N., Sólimo, H.N., 2001. (Liquid + liquid) equilibria of ternary and quaternary systems including 2,2,4-trimethylpentane, benzene, methanol, and water at T= 303.15 K. J. Chem. Thermodyn. 33 (12), 1663–1677. https://doi.org/10.1006/jcht.2001.0865.

Griswold, S.Y., Wong, J., 1952. Phase-equilibria in the acetone-methanol-water system from 100C into the critical region. Chem. Eng. Prog. Symp. Ser. 18–34.

Gross, J., Sadowski, G., 2001. Perturbed-chain SAFT: an equation of state based on a perturbation theory for chain molecules. Ind. Eng. Chem. Res. 40 (4), 1244–1260. https://doi.org/10.1021/ie0003887.

Guo, Y., et al., 2018. Communication: An improved linear scaling perturbative triples correction for the domain based local pair-natural orbital based singles and doubles coupled cluster method [DLPNO-CCSD(T)]. J. Chem. Phys. 148 (1), 011101 https://doi.org/10.1063/1.5011798.

Haghmoradi, A., Chapman, W.G., 2019. Bond cooperativity and ring formation in hydrogen fluoride thermodynamic properties: A two-density formalism framework. J. Chem. Phys. 150 (17) https://doi.org/10.1063/1.5079874.

Haslam, A.J., et al., 2020. Expanding the applications of the saft-γmie group-contribution equation of state: prediction of thermodynamic properties and phase behavior of mixtures. J. Chem. Eng. Data 65 (12), 5862–5890. https://doi.org/10.1021/acs.jced.0c00746.

Huang, S.H., Radosz, M., 1991. Equation of state for small, large, polydisperse, and associating molecules: extension to fluid mixtures. Ind. Eng. Chem. Res. 30 (8), 1994–2005. https://doi.org/10.1021/ie00056a050.

Ito, T., Yoshida, F., 1963. Vapor-liquid equilibria of water-lower fatty acid systems: water-formic acid, water acetic acid and water-propionic acid. J. Chem. Eng. Data 8 (3), 315–320. https://doi.org/10.1021/je60018a012.

Jackson, G., Chapman, W.G., Gubbins, K.E., 1988. Phase equilibria of associating fluids spherical molecules with multiple bonding sites. Mol. Phys. 65 (1), 1–31. https://doi.org/10.1080/00268978800100821.

Kendall, R.A., Dunning, T.H., Harrison, R.J., 1992. Electron affinities of the first-row atoms revisited. Systematic basis sets and wave functions. J. Chem. Phys. 96 (9), 6796–6806. https://doi.org/10.1063/1.462569.

Kenttaemaa, M., Tommila, J., Martti, E., 1959. "Some thermodynamic properties of the system t-butanol + water", in Ann. Acad. Sci. Fenn. Ser. A2, 1–20.

King, M.B., Mubarak, A., Kim, J.D., Bott, T.R., 1992. The mutual solubilities of water with supercritical and liquid carbon dioxides. J. Supercrit. Fluids 5 (4), 296–302. https://doi.org/10.1016/0896-8446(92)90021-B.

Kogan, V.B., Deizenrot, I.V., Kul'dyaeva, T.A., Fridman, V.M., 1956. Solubility in the systems methanol, water, and paraffinic hydrocarbons. Zh. Prikl. Khim. 29, 1387.

Kontogeorgis, G.M., Voutsas, E.C., Yakoumis, I.V., Tassios, D.P., 1996. An equation of state for associating fluids. Ind. Eng. Chem. Res. 35 (11), 4310–4318. https://doi.org/10.1021/ie9600203.

Kontogeorgis, G.M., Yakoumis, I.V., Meijer, H., Hendriks, E., Moorwood, T., 1999. Multicomponent phase equilibrium calculations for water–methanol–alkane mixtures. Fluid Phase Equilib. 158–160, 201–209. https://doi.org/10.1016/S0378-3812(99)00060-6.

Kontogeorgis, G.M., Michelsen, M.L., Folas, G.K., Derawi, S., von Solms, N., Stenby, E.H., 2006. Ten years with the CPA (Cubic-Plus-Association) equation of state. part 2. cross-associating and multicomponent systems. Ind. Eng. Chem. Res. 45 (14), 4869–4878. https://doi.org/10.1021/ie051306n.

Kontogeorgis, G.M., Michelsen, M.L., Folas, G.K., Derawi, S., von Solms, N., Stenby, E.H., 2006. Ten years with the CPA (Cubic-Plus-Association) equation of state. Part 1. pure compounds and self-associating systems. Ind. Eng. Chem. Res. 45 (14), 4855–4868. https://doi.org/10.1021/ie051305v.

Kontogeorgis, G.M., Folas, G.K., Muro-Suñé, N., Roca Leon, F., Michelsen, M.L., 2008. Solvation phenomena in association theories with applications to oil & gas and chemical industries. Oil Gas Sci. Technol. - Rev. L'ifp 63 (3), 305–319. https://doi.org/10.2516/ogst:2008025.

Kontogeorgis, G.M., Folas, G.K., 2009. Thermodynamic Models for Industrial Applications: From Classical and Advanced Mixing Rules to Association Theories. John Wiley & Sons.

Kossmann, S., Neese, F., 2010. Efficient structure optimization with second-order many-body perturbation theory: the rijcosx-mp2 method. J. Chem. Theory Comput. 6 (8), 2325–2338. https://doi.org/10.1021/ct100199k.

Kurihara, K., Minoura, T., Takeda, K., Kojima, K., 1995. Isothermal vapor-liquid equilibria for methanol + ethanol + water, methanol + water, and ethanol + water. J. Chem. Eng. Data 40 (3), 679–684. https://doi.org/10.1021/je00019a033.

Liakos, D.G., Sparta, M., Kesharwani, M.K., Martin, J.M.L., Neese, F., 2015. Exploring the accuracy limits of local pair natural orbital coupled-cluster theory. J. Chem. Theory Comput. 11 (4), 1525–1539. https://doi.org/10.1021/ct501129s.

Lopes, S., Fausto, R., Khriachtchev, L., 2016. Acetic acid-water complex: the first observation of structures containing the higher-energy acetic acid conformer. J. Chem. Phys. 144 (8), pp. https://doi.org/10.1063/1.4942027.

Mac Dowell, N., Llovell, F., Adjiman, C.S., Jackson, G., Galindo, A., 2010. Modeling the fluid phase behavior of carbon dioxide in aqueous solutions of monoethanolamine using transferable parameters with the SAFT-VR approach. Ind. Eng. Chem. Res. 49 (4), 1883–1899. https://doi.org/10.1021/ie901014t.

Marshall, B.D., Chapman, W.G., 2013. Resummed thermodynamic perturbation theory for bond cooperativity in associating fluids. J. Chem. Phys. 139 (21) https://doi.org/10.1063/1.4834637.

Marshall, B.D., Haghmoradi, A., Chapman, W.G., 2014. Resummed thermodynamic perturbation theory for bond cooperativity in associating fluids with small bond angles: Effects of steric hindrance and ring formation. J. Chem. Phys. 140 (16) https://doi.org/10.1063/1.4871307.

Marshall, B.D., 2017. A second order thermodynamic perturbation theory for hydrogen bond cooperativity in water. J. Chem. Phys. 146 (17) https://doi.org/10.1063/1.4982229.

Marshall, B.D., 2019. A resummed thermodynamic perturbation theory for positive and negative hydrogen bond cooperativity in water. J. Phys. Condens. Matter 31 (18). https://doi.org/10.1088/1361-648X/ab03c5.

Mihrin, D., Jakobsen, P.W., Voute, A., Manceron, L., Wugt Larsen, R., 2019. High-resolution infrared synchrotron investigation of (hcn) 2 and a semi-experimental determination of the dissociation energy D0. ChemPhysChem 20 (23), 3238–3244. https://doi.org/10.1002/cphc.201900811.

Mihrin, D., Voute, A., Jakobsen, P.W., Feilberg, K.L., Wugt Larsen, R., 2022. The effect of alkylation on the micro-solvation of ethers revealed by highly localized water librational motion. J. Chem. Phys. 156 (8), 084305 https://doi.org/10.1063/5.0081161.

Müller, G., Bender, E., Maurer, G., 1988. Das dampf-flüssigkeitsgleichgewicht des ternären systems ammoniak-kohlendioxid-wasser bei hohen wassergehalten im bereich zwischen 373 und 473 kelvin. Berichte Der Bunsengesellschaft Für Phys. Chemie 92 (2), 148–160. https://doi.org/10.1002/bbpc.198800036.

Muro-Suñé, N., Kontogeorgis, G.M., Von Solms, N., Michelsen, M.L., 2008. Phase equilibrium modelling for mixtures with acetic acid using an association equation of state. Ind. Eng. Chem. Res. 47 (15), 5660–5668. https://doi.org/10.1021/ie071205k.

Nedić, M., Wassermann, T.N., Larsen, R.W., Suhm, M.A., 2011. A combined Raman- and infrared jet study of mixed methanol-water and ethanol-water clusters. PCCP 13 (31), 14050–14063. https://doi.org/10.1039/c1cp20182d.

Neese, F., Jan. 2018. Software update: the ORCA program system, version 4.0. WIREs Comput. Mol. Sci. 8 (1) https://doi.org/10.1002/wcms.1327.

Neese, F., Wennmohs, F., Hansen, A., Becker, U., 2009. Efficient, approximate and parallel Hartree-Fock and hybrid DFT calculations. a 'chain-of-spheres' algorithm for the Hartree-Fock exchange. Chem. Phys. 356 (1–3), 98–109. https://doi.org/10.1016/j.chemphys.2008.10.036.

Noda, K., Sato, K., Nagatsuka, K., Ishida, K., 1975. Ternary liquid-liquid equilibria for the systems of aqueous methanol solutions Solutions and Propane or n-butane. J. Chem. Eng. Japan 8 (6), 492–493. https://doi.org/10.1252/jcej.8.492.

Panagiotopoulos, A.Z., Willson, R.C., Reid, R.C., 1988. Phase equilibria in ternary systems with carbon dioxide, water and carboxylic acids at elevated pressures. J. Chem. Eng. Data 33 (3), 321–327. https://doi.org/10.1021/je00053a028.

Pemberton, R., Mash, C., 1978. Thermodynamic properties of aqueous non-electrolyte mixtures II. Vapour pressures and excess Gibbs energies for water + ethanol at 303.15 to 363.15 K determined by an accurate static method. J. Chem. Thermodyn. 10 (9), 867–888. https://doi.org/10.1016/0021-9614(78)90160-X.

Perakis, C.A., Voutsas, E.C., Magoulas, K.G., Tassios, D.P., 2007. Thermodynamic modeling of the water + acetic acid + co2 system: the importance of the number of association sites of water and of the nonassociation contribution for the cpa and saft-type models. Ind. Eng. Chem. Res. 46 (3), 932–938. https://doi.org/10.1021/ie0609416.

Phutela, R., Kooner, Z., Fenby, D., 1979. Vapour pressure study of deuterium exchange reactions in water-ethanol systems: equilibrium constant determination. Aust. J. Chem. 32 (11), 2353. https://doi.org/10.1071/CH9792353.

Ribeiro, R.T.C.S., Alberton, A.L., Paredes, M.L.L., Kontogeorgis, G.M., Liang, X., 2018. Extensive study of the capabilities and limitations of the cpa and spc-saft equations of state in modeling a wide range of acetic acid properties. Ind. Eng. Chem. Res. 57 (16), 5690–5704. https://doi.org/10.1021/acs.iecr.8b00148.

Riplinger, C., Pinski, P., Becker, U., Valeev, E.F., Neese, F., 2016. Sparse maps—a systematic infrastructure for reduced-scaling electronic structure methods. II. Linear scaling domain based pair natural orbital coupled cluster theory. J. Chem. Phys. 144 (2), 024109 https://doi.org/10.1063/1.4939030.

Rodriguez, J., Mac Dowell, N., Llovell, F., Adjiman, C.S., Jackson, G., Galindo, A., 2012. Modelling the fluid phase behaviour of aqueous mixtures of multifunctional alkanolamines and carbon dioxide using transferable parameters with the SAFT-VR approach. Mol. Phys. 110 (11–12), 1325–1348. https://doi.org/10.1080/00268976.2012.665504.

Sadlej, J., Mazurek, P., 1995. Ab initio calculations on the water-carbon dioxide system. J. Mol. Struct. (Thoechem) 337 (2), 129–138. https://doi.org/10.1016/0166-1280(95)04132-P.

Schreinemakers, F.A., 1900. Dampfdrücke binärer und ternärer Gemische. Z. Phys. Chem. 35, 459–479.

Sear, R.P., Jackson, G., 1996. Thermodynamic perturbation theory for association with bond cooperatively. J. Chem. Phys. 105 (3), 1113–1120. https://doi.org/10.1063/1.471955.

Sørensen, J.M.A., Pa. 1980.. Liquid – Liquid Equilibrium Data Collection (ternary Systems) Vol. V.

Suresh, S.J., Elliott, J.R., 1992. Multiphase equilibrium analysis via a generalized equation of state for associating mixtures. Ind. Eng. Chem. Res. 31 (12), 2783–2794. https://doi.org/10.1021/ie00012a025.

Takenouchi, S., Kennedy, G.C., 1964. The binary system H2O-CO2 at high temperatures and pressures. Am. J. Sci. 262 (9), 1055–1074. https://doi.org/10.2475/ajs.262.9.1055.

Toedheide, K., Franck, E.U., 1963. Two-phase region and the critical curve in the carbon dioxide-water system at pressures up to 3500 bar. Z. Phys. Chem. 37, 387–401.

Towne, J., Liang, X., Kontogeorgis, G.M., 2021. Application of quantum chemistry insights to the prediction of phase equilibria in associating systems. Ind. Eng. Chem. Res. 60 (16), 5992–6005. https://doi.org/10.1021/acs.iecr.1c00072.

Tsivintzelis, I., Kontogeorgis, G.M., Michelsen, M.L., Stenby, E.H., 2011. Modeling phase equilibria for acid gas mixtures using the CPA equation of state. Part II: binary mixtures with CO2. Fluid Phase Equilib. 306 (1), 38–56. https://doi.org/10.1016/j.fluid.2011.02.006.

Tsonopoulos, C., Prausnitz, J.M., 1970. Fugacity coefficients in vapor-phase mixtures of water and carboxylic acids. Chem. Eng. J. 1 (4), 273–278. https://doi.org/10.1016/0300-9467(70)85014-6.

Tsuzuki, S., Uchimaru, T., Tanabe, K., 1996. Refinement of nonbonding interaction parameters for carbon dioxide on the basis of the pair potentials obtained by mp2/6-311+g(2df)-level ab initio molecular orbital calculations. J. Phys. Chem. 100 (11), 4400–4407. https://doi.org/10.1021/jp952275k.

Tsvintzelis, I., et al., 2012. The Cubic-Plus-Association EoS. Parameters for pure compounds and interaction parameters. Technical Report, Technical University of Denmark.

Valtz, A., Chapoy, A., Coquelet, C., Paricaud, P., Richon, D., 2004. Vapour–liquid equilibria in the carbon dioxide–water system, measurement and modelling from 278.2 to 318.2K. Fluid Phase Equilib. 226, 333–344. https://doi.org/10.1016/j.fluid.2004.10.013.

Von Solms, N., Michelsen, M.L., Passos, C.P., Derawi, S.O., Kontogeorgis, G.M., 2006. Investigating models for associating fluids using spectroscopy. Ind. Eng. Chem. Res. 45 (15), 5368–5374. https://doi.org/10.1021/ie051341u.

Voutsas, E.C., Yakoumis, I.V., Tassios, D.P., 1999. Prediction of phase equilibria in water/alcohol/alkane systems. Fluid Phase Equilib. 158–160, 151–163. https://doi.org/10.1016/s0378-3812(99)00131-4.

Weigend, F., 2002. A fully direct RI-HF algorithm: implementation, optimised auxiliary basis sets, demonstration of accuracy and efficiency. PCCP 4 (18), 4285–4291. https://doi.org/10.1039/b204199p.

Weigend, F., 2006. Accurate Coulomb-fitting basis sets for H to Rn. PCCP 8 (9), 1057. https://doi.org/10.1039/b515623h.

Weigend, F., 2008. Hartree–Fock exchange fitting basis sets for H to Rn. J. Comput. Chem. 29 (2), 167–175. https://doi.org/10.1002/jcc.20702.

Weigend, F., Köhn, A., Hättig, C., 2002. Efficient use of the correlation consistent basis sets in resolution of the identity MP2 calculations. J. Chem. Phys. 116 (8), 3175–3183. https://doi.org/10.1063/1.1445115.

Weller, R., Schuberth, H., Leibnitz, E., 1963. Phasengleichgewichtsmessungen. IV. die phasengleichgewichte dampfförmig/flüssig des systems phenol/n-butylacetat/wasser bei 44,4°C. J. Für Prakt. Chemie 21 (5–6), 234–249. https://doi.org/10.1002/prac.19630210502.

Wertheim, M.S., 1984. Fluids with highly directional attractive forces. i. statistical thermodynamics. J. Stat. Phys. 35, 19–34. https://doi.org/10.1007/BF01017362.

Wertheim, M.S., 1984. Fluids with highly directional attractive forces. II. thermodynamic perturbation theory and Integral equations. J. Stat. Phys. 35, 35–47. https://doi.org/10.1007/BF01017363.

Wertheim, M.S., 1986. Fluids with highly directional attractive forces. iv. equilibrium polymerization. J. Stat. Phys. 42, 477–492. https://doi.org/10.1007/BF01127722.

Wertheim, M.S., 1986. Fluids with highly directional attractive forces. iii. multiple attraction sites. J. Stat. Phys. 42, 459–476. https://doi.org/10.1007/BF01127721.

Wiebe, R., Gaddy, V.L., 1939. The solubility in water of carbon dioxide at 50, 75 and 100°, at pressures to 700 atmospheres. J. Am. Chem. Soc. 61 (2), 315–318. https://doi.org/10.1021/ja01871a025.

Wiebe, R., Gaddy, V.L., 1940. The solubility of carbon dioxide in water at various temperatures from 12 to 40° and at pressures to 500 atmospheres. critical phenomena *. J. Am. Chem. Soc. 62 (4), 815–817. https://doi.org/10.1021/ja01861a033.

Wiebe, R., Gaddy, V.L., 1941. Vapor phase composition of carbon dioxide-water mixtures at various temperatures and at pressures to 700 atmospheres. J. Am. Chem. Soc. 63 (2), 475–477. https://doi.org/10.1021/ja01847a030.

Wormald, C.J, Colling, C.N, Sellars, A.J., 1983. 1983 International gas research conference, proceedings, pp. 1070–1079.

Wolbach, J.P., Sandler, S.I., 1997. Thermodynamics of hydrogen bonding from molecular orbital theory: 2. Organics. AIChE J 43 (6), 1597–1604. https://doi.org/10.1002/aic.690430623.

Wolbach, J.P., Sandler, S.I., 1997. Thermodynamics of hydrogen bonding from molecular orbital theory: 1. Water. AIChE J 43 (6), 1589–1596. https://doi.org/10.1002/aic.690430622.

Wolbach, J.P., Sandler, S.I., 1997. Using molecular orbital calculations to describe the phase behavior of hydrogen-bonding fluids. Ind. Eng. Chem. Res. 36 (10), 4041–4051. https://doi.org/10.1021/ie9607255.

Wolbach, J.P., Sandler, S.I., 1998. Using molecular orbital calculations to describe the phase behavior of cross-associating mixtures. Ind. Eng. Chem. Res. 37 (8), 2917–2928. https://doi.org/10.1021/ie970781l.

Wu, H.S., Hagewiesche, D., Sandler, S.I., 1988. Vapor-liquid equilibria of 2-propanol + water + N, N-dimethyl formamide. Fluid Phase Equilib. 43 (1), 77–89. https://doi.org/10.1016/0378-3812(88)80073-6.

Zawisza, A., Malesinska, B., 1981. Solubility of carbon dioxide in liquid water and of water in gaseous carbon dioxide in the range 0.2-5 MPa and at temperatures up to 473 K. J. Chem. Eng. Data 26 (4), 388–391. https://doi.org/10.1021/je00026a012.